The influence of differently shaped behavioral zones on the shape and structure of fish schools

- Master Thesis -

Jeroen Kuijpers

May 17, 2010

Internal Supervisors:
Prof. dr. L.R.B. Schomaker. Artificial Intelligence, University of Groningen
drs. T. van der Zant. Artificial Intelligence, University of Groningen
External Supervisor:
Prof. dr. C.K. Hemelrijk. Theoretical Biology, University of Groningen
dr. H. Hildenbrandt. Theoretical Biology, University of Groningen
drs. D.A.P. Reid. Theoretical Biology, Univerisity of Groningen

rijksuniversiteit groningen

Abstract

Agent-based models have shown that local interactions between identical agents can, through self-organizational processes, give rise to patterns at a group level that resemble those in animal groups, such as flocking birds or schooling and milling fish. Flocking or schooling is achieved in most models by surrounding the individuals with behavioral (response) zones which induce the individual to avoid agents that are close-by, align with those at mid-range and are attracted to others that are further away. Previous models have shown that circular (2D) and spherical (3D) behavioral zones give rise to elongated schools. There are, however, physiological indications that circular or spherical behavioral zones do not accurately reflect the sensory capabilities of real fish. In addition, the width-height ratios of schools brought about by spherical behavioral zones do not sufficiently resemble empirical measurements of real fish schools.

The present study investigates the effects on school shape and structure of differently shaped behavioral zones in a model of schooling fish. It was found that the school shape in general adopts the shape of the behavioral zone and is additionally influenced by group size and density of the schools. School structure is expressed in terms of the position of the nearest neighbors with respect to the individuals. For stronger attraction the positions of the nearest neighbors are mainly determined by the individuals' blind angle, whereas for weaker attraction the nearest neighbors are most often found at position where the behavioral zones are smallest. Furthermore, this study explains how these spatial structures emerge through measurements of the direction and magnitude of the repulsion and attraction forces experienced by the individuals.

This study is the first to show schools with realistic school structures, i.e. angles towards positions of the nearest neighbors, and school shapes that resemble empirical data in all three dimensions. The schools which most resemble those of real fish result from behavioral zones which extend less in the vertical direction. This might indicate that fish respond more to, or can more easily perceive, conspecifics swimming on the movement plane.

Contents

Chapter 1

Introduction

Everywhere around us there are dynamic group interactions from bacteria to whales, from pedestrians to birds. Interactions between individuals can result in complex spatial patterns. Models are ideal for studying the emergence of these patterns, as behavior is often better understood bottom-up than top-down. Many patterns observed in empirical studies of group behavior can be created in models through self-organization.

Aoki found that effective schooling, like in fish, can be obtained when individuals possess three interaction rules: avoid agents that are close-by, align with those at mid-range, and approach others that are further away [1]. These rules form the basis for most models of movement swarms. By adding object avoidance to these three rules Reynolds created natural looking flocks of artificial birds [43]. Huth and Wissel were the first ones to compare empirical measurements of fish schools with results from their model [29] (figure 1.1).

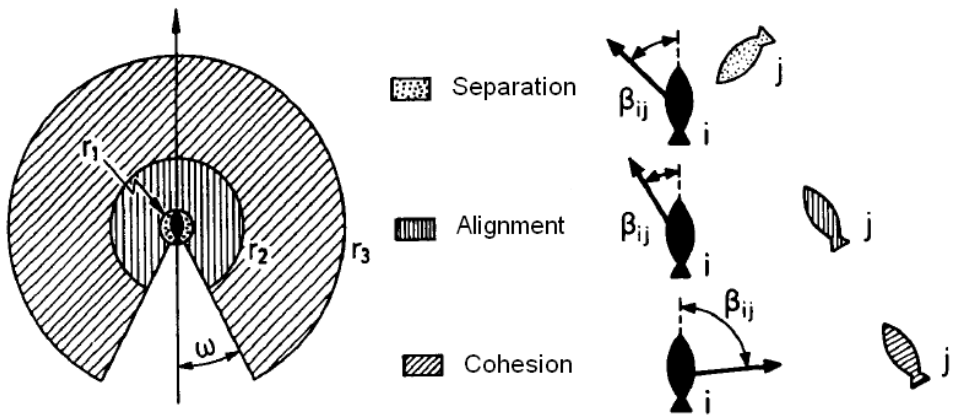

Figure 1.1: A schematic overview of circular behavioral zones with a rear blind angle. β_{ij} illustrates the behavioral response to an agent within the corresponding behavioral zone. This figure is an modification of a figure previously published by Huth and Wissel [29].

Multiple models have shown an oblong school[1] can emerge solely as a side-effect of the three aforementioned behavioral responses, i.e. separation, alignment and cohesion [34, 25, 23]. The concentric behavioral response zones to which the separation, alignment and cohesion behavior apply are usually circular (2D) or spherical (3D). Hemelrijk and Hildenbrandt show that the

[1] A school of which the length is bigger than the width

emergence of the oblong shape in their model arises because agents with spherical behavioral zones decelerate to avoid other agents. This results in an oblong school of which the width is slightly bigger than the height. Schools of real fish are oblong, but are additionally much wider than they are high (table 1.1).

School shape Length : Width : Height	Species	Study by
2.1 : 1.7 : 1	pilchard	Cullen et al. 1965
3 : 2 : 1	minnow	Pitcher 1973
4 : 2 : 1	muller	Breder 1959
5.6 : 2.1 : 1	saithe	Pitcher and Partridge 1979
6 : 3 : 1	saithe	Partridge et al. 1980
3 : 3.1 : 1	herring	Partridge et al. 1980
2 - 10 : 4 : 1	cod	Partridge et al. 1980

Table 1.1: Overview of the relative dimensions of fish school shapes per species. For most fish species it holds that school length > width > height.

The three-dimensional shape, especially the flatness, of the schools is often overlooked or not measured in fish models. Many models are even two-dimensional [28, 29, 14, 34, 25]. The three-dimensional structure of the schools can be measured through the distributions of the bearing and elevation angle, which indicate the direction to the nearest neighbors in the horizontal and vertical plane respectively. The bearing and elevation angle are frequently measured in schools of real fish. In simulation studies, however, bearing and elevation angles are rarely published and those that are published do not resemble empirical measurements [27]

The present research investigates the relation between the shape of the behavioral zones and the emerging school shape and structure in a three-dimensional model of schooling fish. We hypothesize that changing the shape of the behavioral zones will influence the shape and structure of the school and that an ellipsoidal behavioral zones will bring about more realistic schools than spherical behavioral zones.

The behavioral zones symbolize the sensory capabilities *and* the behavioral responses of an individual. There are indications that spherical behavioral zones do not sufficiently reflect the sensory capabilities of a fish. Fish achieve schooling using vision and series of hydrodynamic sensors, called the lateral line [37], which can detect the speed and heading of neighboring conspecifics [18, 17]. The lateral line mainly provides avoidance and alignment [40] and runs along the body of the fish (figure 1). This could indicate that the shape of the separation and alignment zones should more resemble that of a fish.

Figure 1.2: Lateral line of a cod runs along the side of the body, previously published by Denton and Gray [18].

Furthermore, spherical behavioral zones might not realistically imitate the behavioral response of a real fish. Spherical behavioral zones indicate that an agent is equally influenced all neighbors whether they swim on the same movement plane or above (dorsal side) or below (ventral side) the focal agent. Fish produce a vortex wake by undulating, which can be exploited by other fish to decrease energy costs of locomotion [50]. A fish cannot exploit the

vortex wakes produced by neighboring fish swimming above or below them, hence these neighbors presumably have a smaller influence on the behavior of a fish. Flatter behavioral zones would better reflect this difference.

Little research has been done on the effects of differently shaped behavioral zones. Kunz and Hemelrijk built a two-dimensional model in which they compared, among other things, the spatial properties of a school of agents with circular and elliptical behavioral zones [34]. The elliptically shaped behavioral zones, elongated in the traveling direction, were hypothesized by the authors to be a more natural representation of the sensory capabilities of real fish. However, their agents with elliptical behavioral zones bring about less realistic schools, i.e. the schools are wide and not oblong. The authors further show that elliptical behavioral zones give rise to relative smaller lateral distances between individuals and thus to denser schools. It should be noted that these results cannot be attributed solely to the influence of shape of the behavioral zones, because the area of the elliptical separation and alignment zones are also smaller that the circular ones.

A mechanistic approach to investigate schooling behavior serves multiple purposes. First of all, it gives insights into how fish school and how certain spatial organizations emerge, which cannot be deduced by merely observing them. Collective movement of animals may be based on the same principles. A relation between shape of behavioral zones and the spatial properties of a school could therefore easily be extrapolated and used in models of other animals, like for example a model of starlings [26], pedestrians [22], locusts [4] or wildebeests [15].

Mechanisms that control shape and/or structure of any group of self-propelled particles are not only useful for modeling animal movement, but could also be useful in many real-world application. Artificial Intelligence researchers and engineers favor distributed approaches over a single complex system, as a group of self-organizing agents provide solutions that are cheap, fault tolerant, fast and simple [51]. The field of swarming robotics deals with the coordination of groups of robots. Distributed sensing and mapping of the environment, and problems involving finding particular items, such as mines, survivors or oil spills, are typical problems which are studied using swarming robotics.

The swarm shape and structure are vital aspects of these problems. A loose structure can provide a better coverage of the environment, whereas denser formation provides more connectivity and redundancy [31]. Certain formations, like a line or wedge formation, could improve efficiency when exploring or mapping an environment [9].

Top down control mechanisms which choreograph the movements of all agents are too computationally expensive and generally not able to deal with real-life situations. Control mechanism based on self-organization are simple and robust, because their spatial patterns are a side-effect of interactions between the agents. These simple local interactions can give rise to formations where certain types of agent occupy the center and other types the periphery [45, 25] or formations where agents adopt lattice or square patterns [47]. Mechanisms proposed to control the shape of a group [5, 32], however, are still complex and computationally expensive as they for a large part control the shape of the school in a top-down manner rather than letting it emerge. Knowing the relation between shape of the behavioral zones and swarm shape provides us with tools to control the shape and structure swarm without having to calculate the movement of each agent. This could, for example, be the basis of a simple control mechanism for large groups of autonomous underwater, aerial, or space vehicles.

The present study thus aims to get schools of agents that resemble those of real fish, but also to get a general understanding of group behavior, i.e. how the shape and structure of movement swarms are influenced by differently shaped behavioral zones. The various shapes of behavioral zones are not directly based on the sensor capabilities and behavioral responses of real fish, because the current understanding of fish is insufficient to choose a specific realistic shape of the behavioral zones beforehand. We therefore run experiments with multple (i.e. 7) different shapes of behavioral zones, during which the school shape and school structure will be measured. The results obtained with the traditional spherical shape serve as a null-model. A comparison will be made with empirical schooling data, to investigate what shape of behavioral zones bring about schools that resemble real fish schools.

Chapter 2

Methods

2.1 The model

This model is an adapted version of a model originally created by H. Hildenbrandt as described in [23]. Modifications concern variations in shape of behavioral zones and measurements such as school volume. The model contains self propelled artificial fish which interact with other agents within a homogeneous 3D world. An agent can interact with multiple agents at once through three behavioral responses, namely separation, alignment and cohesion (figure 2.1*b*). An agent is repulsed by the agents in the separation zone, aligns with those in the alignment zone and is attracted to agents in the cohesion zone. The behavioral zones overlap, which means that the response of an agent to one neighbor can be a combination of multiple behaviors, i.e. separation, alignment or cohesion. This reflects that fish use different sensory systems (lateral line and visual system) to school, which are coupled to different behavioral responses [40].

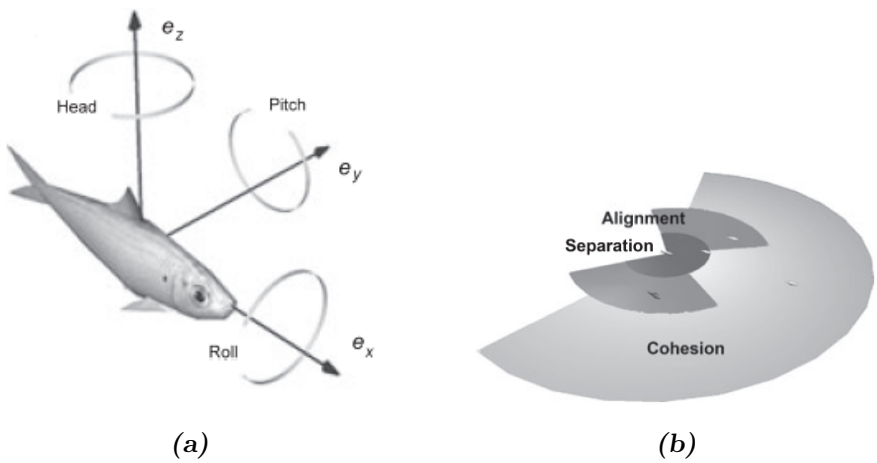

Figure 2.1: a) The local coordinate system of an agent, and the three principle axes over which agent can change its orientation. b) A schematic representation of the different behavioral zones of an agent, originally published by Hemelrijk and Hildenbrandt [23]. Note that the alignment zone in this figure has an additional frontal blind angle. No frontal blind angles are used in this present study.

The agents in the present model have a blind angle at the rear, in which other agents can not be perceived. Hemelrijk and Hildenbrandt used an additional frontal blind angle in the

alignment zone (figure 2.1b) [23]. The alignment zone in the present study does not have a frontal blind angle, because many fish species have a lateral line system on their head (figure 2.2), which enables fish to detect hydrodynamic pressure waves coming from frontal directions.

The new positions of all individuals are updated each time step Δt. Each agent has an position $\vec{p}$, speed v and orientation $\vec{e}_x$, $\vec{e}_y$, $\vec{e}_z$ symbolizing respectively the for-, side- and upward directions. An agent can change its orientation by rotating over these three axes (figure 2.1a), or accelerate or decelerate, similar to the agents in Reynolds' model [43]. The behavior of an agent is based on the position and orientation of its neighbors. The behavioral response to a neighbor is determined by the type of behavioral zones, i.e. separation, alignment or cohesion zone (figure 2.1b).

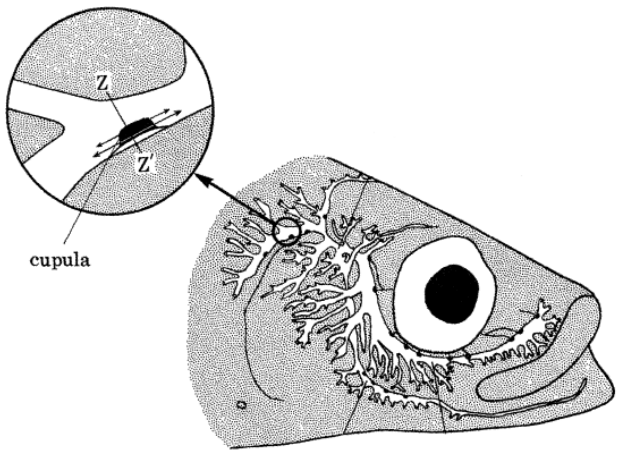

Figure 2.2: The lateral line system on the head of a sprat. The cupulae contain neuromasts which are excited when the cupulae are bended with regards to their base, due to the hydrodynamic flows in the lateral line canals. This figure is previously published by Denton and Gray [18].

Like most models of schooling, the agents in this model are represented by points in space. Therefore, it is possible for agents to come very close to each other, even with a separation behavior, while this obviously is not possible for real fish. A collision avoidance behavior makes sure that the distance between agents does not become too small. Unlike other social forces, the collision avoidance behavior only becomes active occasionally. The collision avoidance behavior will be discussed in detail later on in this section.

The steering force determines the new position of the agent through Newton's laws of motion, i.e. $\vec{F} = m\vec{a}$. The steering force consists of the sum of the social steering forces, i.e. separation, alignment, cohesion, collision avoidance, plus additional random noise and forces which facilitate speed control and correction of unnatural body orientations. All the social forces are weighted by the corresponding factors w_s, w_a, w_c and w_{ca}, indicating the influence of this behavior on the steering force (table 2.1). An agent can only react to its neighbors once per a certain period of time, called the reaction period. This period is randomized after each response ($50 \pm 6.25ms$) to imitate the variations in processing speeds of sensory information of real fish.

The separation force is responsible for the space between the agents. An individual i perceives a separation force, $\vec{f}_{si}$, in the opposite direction of the average direction to all the neigh-

bors, n_s, in its separation zone. The influence of a neighbor on the direction of the separation force, $\vec{d}_{si}$ is weighted with the squared euclidean distance[1] between the agents, $||\vec{px}_{ij}||^2$, as the closest neighbor should be avoided most. The separation force is in that view similar to Newton's law of universal gravitation, although the separation force works in the opposite direction. This implementation of the separation force is identical to repulsion behavior in Reynolds' model [43].

Unlike Reynolds' agents, the agents in the present model use differently shaped behavioral zones. The vector of focal agent i to the neighbor j, $\vec{p}_{ij}$, is therefore first transposed into local space[2] and scaled with the shape of the separation zone. The matrix $\mathbf{E}$ contains the vectors $\vec{e}_x$, $\vec{e}_y$ and $\vec{e}_z$ which indicate for-, side- and upward orientation of the focal agent i. $\mathbf{E}$ is used to transpose $\vec{p}_{ij}$ into local space. The matrix $\mathbf{F}$ is used to scale the separation response, $\vec{f}_{si}$, with the shape of the separation zone. $\mathbf{F}$ contains the inverse of the radii of the separation zone in the for-, side- and upward direction (L, W and H). The scaled vector to neighbor j, $\vec{px}_{ij}$, is obtained by multiplying the matrices $\mathbf{E}$ and $\mathbf{F}$ with the unscaled vector (in global space) $\vec{p}_{ij}$. The magnitude of $\vec{px}_{ij}$, is thus equal everywhere on the boundary of the separation zone.

$$\vec{p}_{ij} = \vec{p}_j - \vec{p}_i \tag{2.1}$$

$$\mathbf{E} = \begin{bmatrix} \vec{e}_x \\ \vec{e}_y \\ \vec{e}_z \end{bmatrix} \tag{2.2}$$

$$\mathbf{F} = \begin{bmatrix} L^{-1}\, max\{L,W,H\} & 0 & 0 \\ 0 & W^{-1}\, max\{L,W,H\} & 0 \\ 0 & 0 & H^{-1}\, max\{L,W,H\} \end{bmatrix} \tag{2.3}$$

$$\mathbf{S} = \mathbf{E}\,\mathbf{F} \tag{2.4}$$

$$\vec{px}_{ij} = \mathbf{S}^{-1}\, \vec{p}_{ij} \tag{2.5}$$

$$\vec{d}_{si} = -\frac{1}{n_s} \sum_{j=1}^{n_s} \frac{\vec{px}_{ij}}{||\vec{px}_{ij}||^2} \tag{2.6}$$

$$\vec{f}_{si} = w_s \frac{\vec{d}_{si}}{||\vec{d}_{si}||} \tag{2.7}$$

The orientations of fish in traveling schools are well-known to be highly polarized. The polarization in this model is predominantly obtained through the alignment behavior. An individual i perceives an alignment force, $\vec{f}_{ai}$, which rotates the individual (and its forward vector $\vec{e}_{xi}$) is more parallel to the average forward vector of all neighbors n_a in the alignment zone. The directional vector $\vec{d}_{ai}$ indicates the direction of the alignment force. Note that $\vec{d}_{ai}$ is not an unit vector. It is therefore divided by its own length $||\vec{d}_{ai}||$ in equation 2.9. The same holds for the directional vectors of the other behavioral responses: $\vec{d}_{si}$, $\vec{d}_{ci}$ and $\vec{d}_{cai}$.

[1] according to the L^2 norm

[2] relative to the orientation of the agent i

$$\vec{d}_{ai} = -\frac{1}{n_a}\sum_{j=1}^{n_a}\vec{e}_{xj} \tag{2.8}$$

$$\vec{f}_{ai} = w_a\frac{\vec{d}_{ai} - \vec{e}_{xi}}{||\vec{d}_{ai} - \vec{e}_{xi}||} \tag{2.9}$$

The attraction between the individuals is facilitated through the cohesion behavior. An individual i perceives a cohesion force $\vec{f}_{ci}$, towards the center of gravity of all the neighbors n_c in the cohesion zone. The direction $\vec{d}_{ci}$ to the center of gravity is obtained by calculating the mean position of the neighbors.

$$\vec{d}_{ci} = -\frac{1}{n_c}\sum_{j=1}^{n_c}\frac{\vec{p}_{ij}}{||\vec{p}_{ij}||} \tag{2.10}$$

$$\vec{f}_{ci} = w_c\frac{\vec{d}_{ci}}{||\vec{d}_{ci}||} \tag{2.11}$$

Furthermore, an individual i perceives an collision avoidance force $\vec{f}_{cai}$ steering away from the point of an eventual 'collision'. Thus unlike other social forces, the collision avoidance behavior only becomes active occasionally. An individual compares its trajectory to the estimated path (based on the current velocity) of neighbor j when it is not further away than 1 Body Length (BL) and neighbor j is in front of the focal agent, i.e. the angle of the direction to the neighbor with respect to the heading of individual i should be smaller than 60° (collision maximum angle). An individual i anticipates a collision when the shortest distance between the estimated paths is smaller than 0.5 BL (panic radius, see table 2.1) *and* both agents reach this point of closest approach within 1.0 second (collision time). The shortest distance between the two paths, and the corresponding positions of the agents at the point of closest approach, $\vec{p1}_{ij}$ and $\vec{p2}_{ij}$, are calculated using the ray-ray intersection test [21]. The direction $\vec{d}_{cai}$ of the collision avoidance force $\vec{f}_{cai}$ is the negative vector from the estimated position of focal individual i, $\vec{p1}_{ij}$, to its neighbor j, $\vec{p2}_{ij}$, at the time of collision. In theory an agent can anticipate collisions with multiple neighbors, n_{ca}.

$$\vec{p'}_{ij} = -(\vec{p2}_{ij} - \vec{p1}_{ij}) \tag{2.12}$$

$$\vec{d}_{cai} = -\frac{1}{n_{ca}}\sum_{j=1}^{n_{ca}}\frac{\vec{p'}_{ij}}{|\vec{p'}_{ij}|^2} \tag{2.13}$$

$$\vec{f}_{cai} = w_{ca}\frac{\vec{d}_{cai}}{||\vec{d}_{cai}||} \tag{2.14}$$

The size of the behavioral zones is dependent on the local density. This imitates sensory obstruction in real fish schools. The more neighbors an individual perceives, $n(t)$, the shorter its perception range $R(t)$ will become. Not shrinking the perception range of an individual with increasing density means that the number of interaction partners will increase to an unrealistic number. Furthermore, empirical evidence in starling flocks suggests that individuals interact

with almost a fixed number of neighbors [3]. The new perception range $R(t+\Delta t)$, is obtained by taking the linear interpolation of the current radius $R(t)$ and the density dependent term $R'(t)$. This makes sure that the change in perception range is gradual. The parameter n_i governs the smoothness of the adaptation. The number of agents in the perception range at a given moment $n(t)$ and the influence of neighbor w_n determine $R'(t)$.

$$R'_i(t) = R_{max} - w_n\, n(t) \tag{2.15}$$

$$R_i(t+\Delta t) = max\{R_{min}, (1-n_i\Delta t)\, R(t) + n_i\Delta t\, R'(t)\} \tag{2.16}$$

The separation, cohesion and collision avoidance forces can also speed up or slow down an individual, although each individual has a preferred cruising speed v_0. Whenever an individual swims faster or slower than its preferred speed, it perceives a compensating force $\vec{f}_{speed}$ that reduces the deviation from v_0. The 'relaxation time' τ corresponds to the time it takes an individual to return to its preferred cruising speed.

$$\vec{f}_{speedi} = \frac{1}{\tau}\,(v_0 - v)\,\vec{e}_{xi} \tag{2.17}$$

Real fish almost never show large pitch angles, i.e. rotations over the sideways vector $\vec{e}_y$ (figure 2.1a), over longer periods of time. Furthermore, real fish are never observed to roll, i.e. rotation over the forward vector $\vec{e}_x$. An individual i therefore perceives a pitch control force $\vec{f}_{pci}$ and a roll control force $\vec{f}_{rci}$ that rotate the individual to a horizontal orientation. The vector z is a unit vector indicating the upward direction in the global coordination system.

$$\vec{f}_{pci} = -w_{pc}(\vec{e}_{xi}\cdot z)\, z \tag{2.18}$$

$$\vec{f}_{rci} = -w_{rc}(\vec{e}_{yi}\cdot z)\, z \tag{2.19}$$

A random vector $\vec{f_{rand}}$, with magnitude w_{rand}, is added to the sum of all the forces to add a stochastic influence to the steering behavior. This, reflects sensory error and undefined external or motivational influences. An individual eventually perceives a steering force $\vec{f_{steeri}}$ which is the sum of all the forces above. The steering force is truncated to f_{max} if the magnitude of $\vec{f_{steeri}}$ exceeds f_{max}. This prevents the steering force of an individual to get unrealistically large and causes the school to be more stable.

$$\vec{f}_{steeri} = \vec{f}_{si} + \vec{f}_{ai} + \vec{f}_{ci} + \vec{f}_{cai} + \vec{f}_{speedi} + \vec{f}_{pci} + \vec{f}_{rci} + \vec{f}_{randi} \tag{2.20}$$

This steering force is applied during, and remains unchanged throughout, the number of time steps Δt within the duration of one reaction time.

Parameter	Unit	Symbol	Value(s) explored
Number of individuals	1	N	50, 250, 750, 1500
Time step	ms	Δt	10
Reaction time	ms	-	50
Reaction time deviation	ms	-	± 6.25
Cruise speed	BL/s	v_0	3.0
Zone of separation			
Minimum radius	BL	R_{min}	1.1
Radii	BL	-	see shapes, table 2.2
Rear blind angle	Degrees	-	90
Zone of alignment			
Radii	BL	-	see shapes, table 2.2
Rear blind angle	Degrees	-	90
Zone of cohesion			
Radius	BL	-	12 (adaptive)
Rear blind angle	Degrees	-	90
Collision Avoidance			
Collision Radius	BL	-	1.0
Collision Time	s	-	1.0
Collision Angle	Degrees	-	120
Panic Radius	BL	-	0.4
Weights			
Separation	$BL^2\,BM/s^2$	w_s	10
Alignment	$BL^2\,BM/s^2$	w_a	8
Cohesion	$BL^2\,BM/s^2$	w_c	9
Collision avoidance	$BL^2\,BM/s^2$	w_{ca}	10
Pitch control	$BL^2\,BM/s^2$	w_{pc}	2
Roll control	$BL^2\,BM/s^2$	w_{rc}	5
Random noise	$BL^2\,BM/s^2$	w_{rand}	1
Relaxation time	s	τ	0.2
Maximum force	$BL^2\,BM/s^2$	f_{max}	2.5

Table 2.1: Overview of the model parameters. These parameters are based on the values used in research by Hemelrijk and Hildenbrandt [23]. Parameters were adjusted such that all the differently shaped behavioral zones bring about schools with realistic nearest neighbors distances which do not disperse into multiple schools. Body Length (BL) is used as a unit of length and Body Mass (BM) as a unit of mass.

2.2 Shape of behavioral zones

Behavioral zones	Separation zone			Alignment zone			Relative dimensions		
	L	W	H	L	W	H	L'	W'	H'
Spherical	1.50	1.50	1.50	5.00	5.00	5.00	1.00	1.00	1.00
High	1.35	1.35	1.80	4.50	4.50	6.00	0.75	0.75	1.00
Flat	1.93	1.93	0.96	6.44	6.44	3.22	1.00	1.00	0.50
Wide	1.35	1.80	1.35	4.50	6.00	4.50	0.75	1.00	0.75
Narrow	1.66	1.24	1.66	5.55	4.16	5.55	1.00	0.75	1.00
Long	1.92	1.44	1.44	6.38	4.79	4.79	1.00	0.75	0.75
Short	1.25	1.67	1.67	4.178	5.57	5.57	0.75	1.00	1.00

Table 2.2: The radii for the different shapes of separation and alignment zones. The relative dimensions (L', W' and H') are obtained by dividing the radii of a particular behavioral zone by its largest dimension. The volumes of the separation and alignment zones are the same for every shape of behavioral zones. These calculations are explained in the appendix, section A.1.

We study the influence of the shape of behavioral zones by running experiments with 7 differently shaped behavioral zones (figure 2.3 - 2.9). Note that only the separation and alignment zone obtain different shapes. The cohesion zone remains spherical (with a blind angle at the rear), because attraction among individuals is mainly facilitated through vision. Repulsion and alignment, on the other hand, are predominately achieved through the lateral line [40].

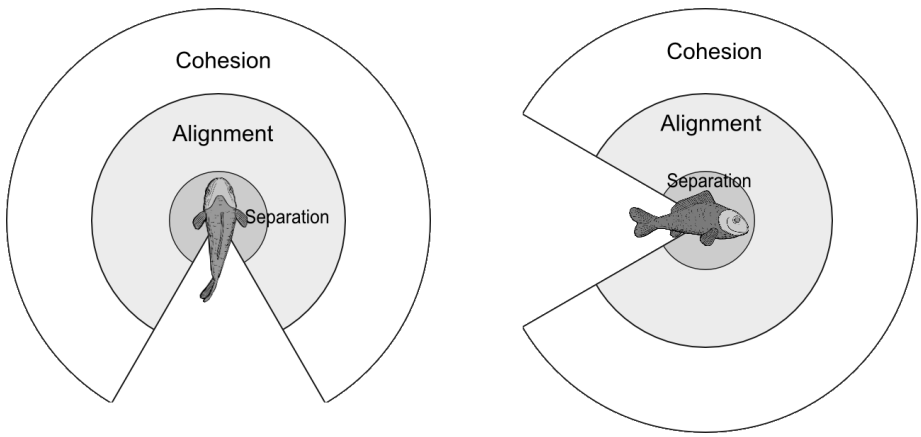

(a) Top-down view ***(b)*** Side view

Figure 2.3: A schematic overview of the Spherical behavioral zones. The behavioral zones displayed here (and below) are an approximation of the used behavioral zones. The exact measurements of the zones can be found in table 2.2.

A deviation of 25% in length of one or more radii of a behavioral zone, i.e. the separation and alignment zone, is enough to get obvious changes in school shape and structure. Further deviating from the spherical shape of behavioral zones in some cases led to schools splitting up into multiple schools. As the number of individuals affect the spatial properties of the school, only measurements of schools are used that did not split up. The zones deviate in all main

directions from a spherical shape to get a good insight on the influence of shape of behavioral zones in general. After the various shapes of the behavioral zones were determined, the relative dimensions of the radii were calculated. The absolute size of the radii of the behavioral zones were calculated such that the volumes of the behavioral zones are equal for each shape. For example, the separation zone of the Spherical behavioral zones has the same volume as the separation zone of the Flat behavioral zones. This means we can attribute changes in spatial properties of the school solely due to the shape of zones.

When calculating the volume which produces a behavioral response, the blind angle has to be taken into account as no behavioral response is invoked to neighbors which swim in the blind angle. All the agents have the same blind angle, but the volume of the blind angle differs per shape of the behavioral zones. Thus the volume (of the active part) of the behavioral zones as well. We calculated the radii of the behavioral zones for which it holds that the volumes of the behavioral zones are equal, because compensating by altering the blind angle per shape of the behavioral zones is not favorable. A difference in the angle of a blind area will result in different behavior, which makes it harder to investigate the influence of the shape. The calculations of the volume of the blind angle and the radii of the behavioral zones can be found in the appendix section A.1.

A schematic overview of:

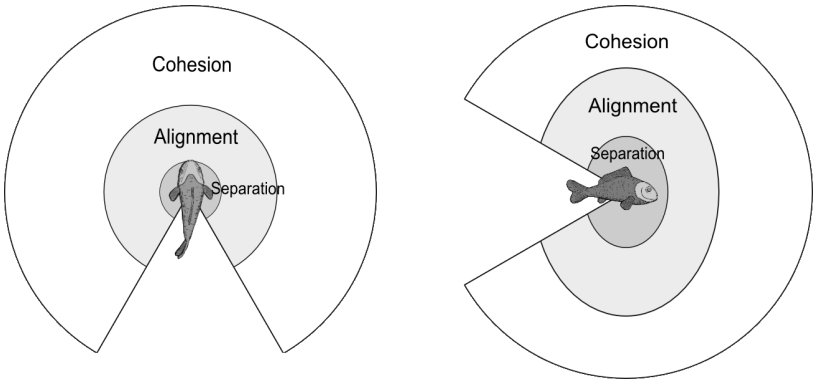

(a) Top-down view ***(b)*** Side view

Figure 2.4: High behavioral zones

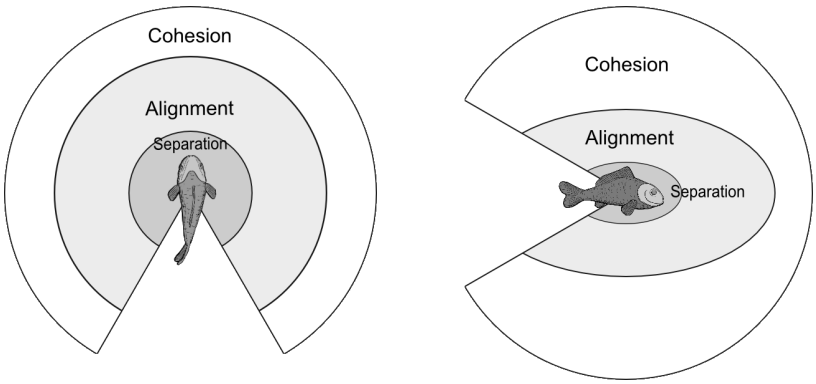

(a) Top-down view ***(b)*** Side view

Figure 2.5: Flat behavioral zones

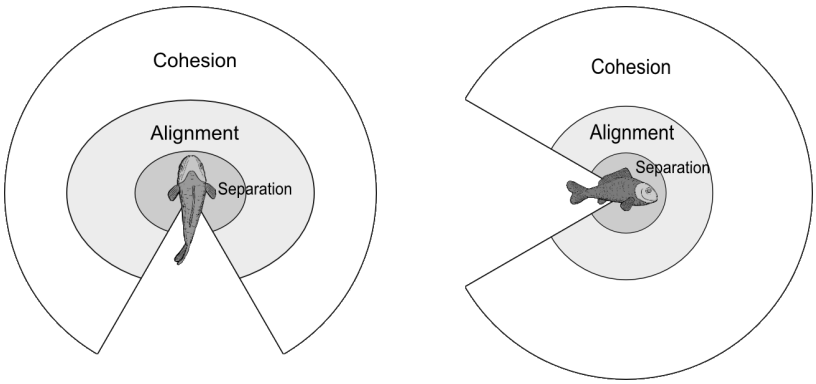

(a) Top-down view ***(b)*** Side view

Figure 2.6: Wide behavioral zones

A schematic overview of:

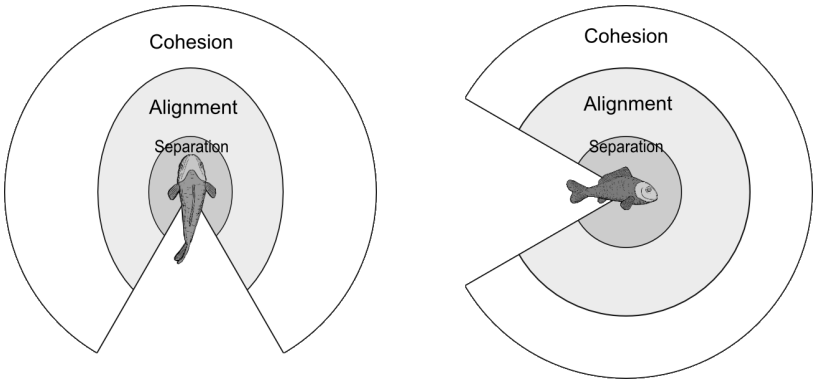

(a) Top-down view ***(b)*** Side view

Figure 2.7: Narrow behavioral zones

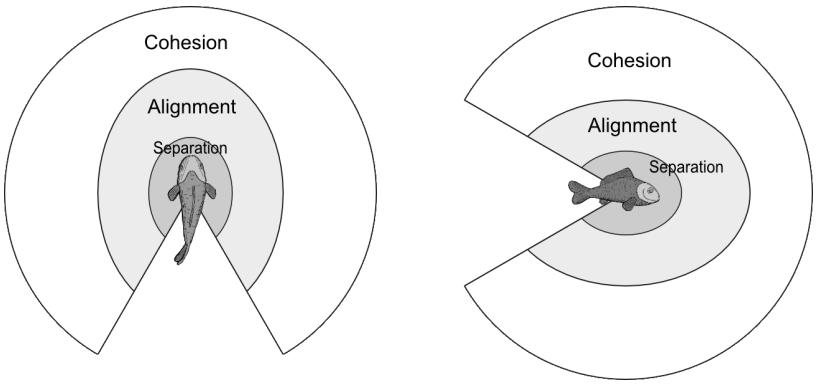

(a) Top-down view ***(b)*** Side view

Figure 2.8: Long behavioral zones

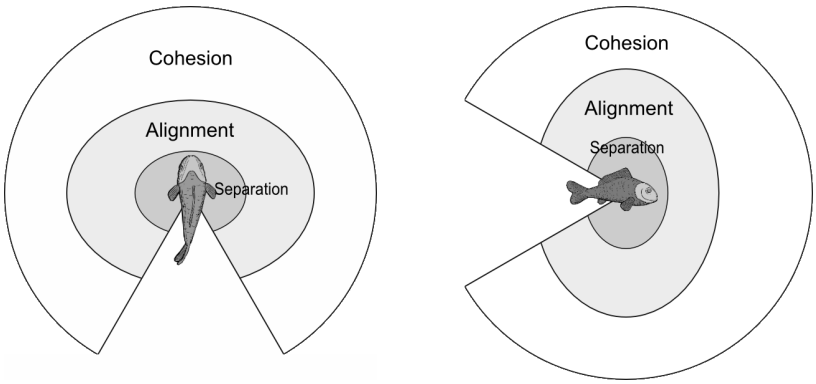

(a) Top-down view ***(b)*** Side view

Figure 2.9: Short behavioral zones

2.3 Experiments

The model is stochastic in the steering forces and reaction time of the agents. School shape and structure are therefore measured over multiple (i.e. 9) runs. Before each run, individuals are assigned to a random position within a sphere. Larger schools can take up to 2.5 minutes to achieve a stable school. The recording starts after 3 minutes and lasts for 6 minutes, during which measurements are performed every 0.75 second. We perform runs with schools containing: 50, 250, 750 and 1500 individuals, similar to the groupsizes in the research by Hemelrijk and Hildenbrandt [23].

2.3.1 Measurements

The effects of differently shaped behavioral zones on the shape of the school are measured using the dimensions of a bounding box which surrounds a school and is aligned to the average heading of all agents. The oblongness of a school can therefore be measured by dividing the length of the bounding box by the width. The flatness of a school is measured by dividing the height of the bounding box by the width.

Various features of school structure can be measured. The main focus in the present study with regards to the school structure lies in the distributions of bearing and elevation angles. The angles towards the nearest neighbor, with respect to the heading of the focal agent, projected on the horizontal and vertical plane are called respectively the bearing and elevation angle (figure 2.10). Bearing angles ranges from 0° (in front) to 180° (at the rear) and elevation angles range from −90° (below) to 90° (above).

We, furthermore, measure the average school speed and the density of the school. Two different density measures are used. Firstly, a global measure of density called the packing density, which is the number of agents divided by school volume. Secondly, the nearest neighbor distance (NND) is used, which is a local measure of density as it measures the average density (or distance to the nearest neighbor) perceived by the individuals [30].

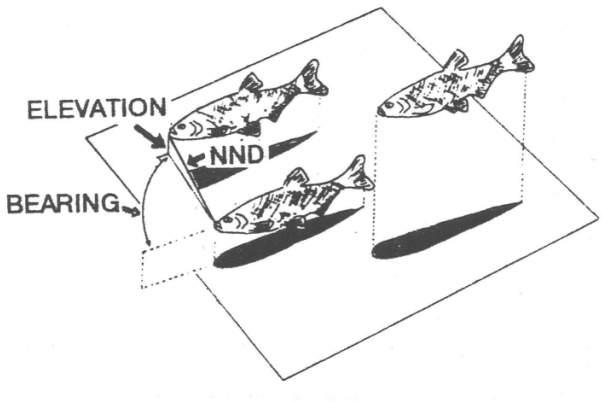

Figure 2.10: The bearing and elevation angles describe the position of the nearest neighbor. The bearing angle is the angle towards the nearest neighbor projected on the horizontal plane and ranges from 0° (in front) to 180° (at the rear). The elevation angle is the angle projected on the vertical plane and has a range of −90° (below) till 90° (above). This figure is previously published by Huth in [27].

2.3.2 Measuring school volume

There are several ways to measure, or estimate, the volume of a school. Pitcher and Partridge measure school volume of schools of real fish by assuming that the school shape resembles an ellipsoid [42]. This method will not suffice considering schools may contain concavities. A more complex solution, called α-shape algorithm, involves carving a convex hull for concavities with a predefined sphere [19, 10]. However, this method cannot deal with non-convex school shapes, like a torus [15], and finding the right size for the sphere can be problematic.

This study proposes another way to measure the volume of a school (V_{school}) which is simple, fast and can deal with non-convex school shapes and concavities. By dividing the bounding box into cells with a similar cell size (cs), we can count the number of cells occupied by an individual (oc) and calculate the volume of the school.

$$V_{school} = cs^3 \; oc \tag{2.21}$$

The difficult part is finding the cell size which gives a reliable estimate of the school volume. Small cell-sizes bring about smaller school volumes and large cell-sizes larger school volumes (figure 2.11), but what cell-size gives an accurate measure of school volume? Schools in general would benefit from a small cell size, because this will keep the edge-effect low. The edge-effect is the error caused by occupied cells located on the edge of the school. Part of these cells lie outside the school but are used nonetheless because the whole volume of the cells are taken into account. The volume of the school is therefore overestimated. Small cell sizes would reduce the edge-effect, but the cell sizes should evidently not be too small. Considering we want to obtain the volume of the school, gaps or unconnected cells are undesirable as this would cause the volume to be too low (figure 2.11a).

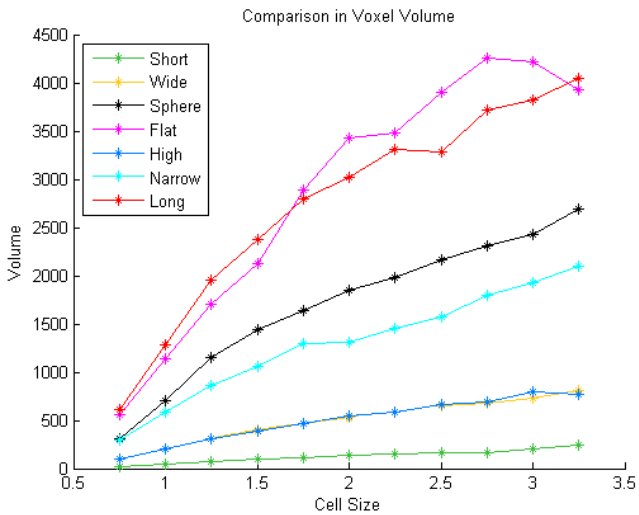

Figure 2.11: The estimated volume of the school grows with the magnitude of the cell-size. Care should thus be taken into selecting the right cell-size.

The maximum number of occupied cells that are connected in one group is calculated and compared against the total number of cells occupied by all individuals. The cells are big enough

to be used as a reliable measure for volume if the number of occupied cells that are connected is equal or close to the total number of occupied cells. A three-dimensional Von Neumann neighborhood was used to determine whether cells are connected or not, which means that only orthogonal (and not diagonal) connections of occupied cells are used (figure 2.12).

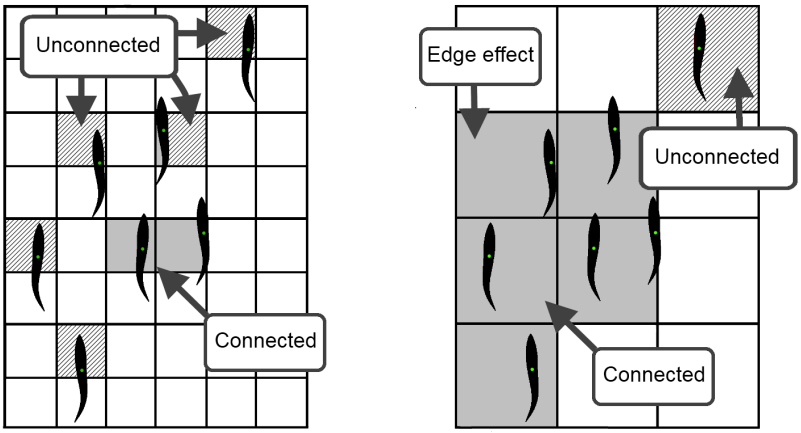

(a) Cell grid with a small cell-size ***(b)*** Cell grid with a large cell-size

Figure 2.12: A 2D example of voxel-based school volume estimation with Von Neumann neighborhood. A Von Neumann neighborhood implies that only perpendicular cells can be connected. a) Too small cell-size, only 2 out of 7 occupied cells are connected. b) The cell-size seems large enough since 6 out of 7 cells are connected. The larger cell-size gives rise to larger edge-effects.

An experiment was performed to see whether the same cell-size could be used for schools brought about by different shapes of behavioral zones and school with different group sizes. The experiment showed that for all schools the number of occupied cells with neighboring occupied cells is equal or close to the total number of occupied cells for a cell-size of 1.25 Body Length (figure 2.13), despite the differences in school shape.

Unoccupied cells within the school would cause an underestimation of volume of the school. The cell grid is not explicitly tested for holes, because the center of the school is denser than the periphery (Appendix, figure A.3).

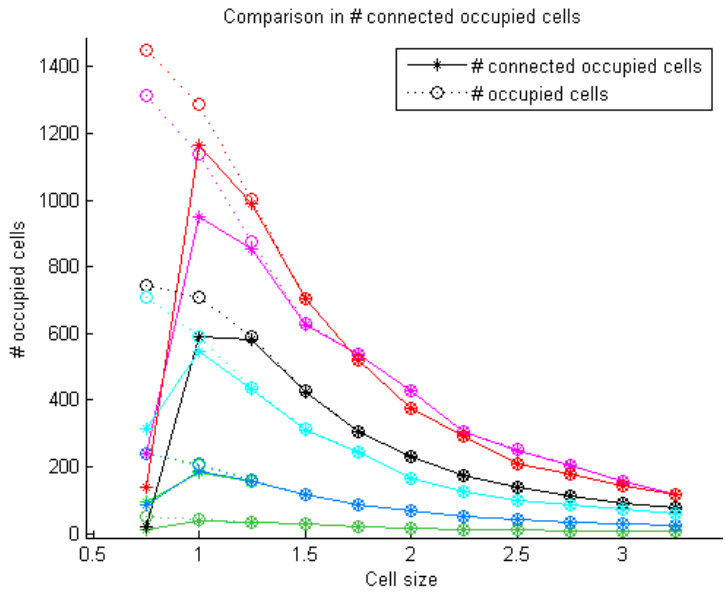

Figure 2.13: The number of connected occupied cells using 3D Von Neumann neighborhood (solid lines) versus the total number of occupied cells (dashed lines), for different cell-sizes. Most occupied cells are connected when a cell-size of 1.25 Body Length (BL) or larger is used. A cell-size 1.25 BL is thus large enough to make a reliable estimate of the volume of the school.

Chapter 3

Results

3.1 Spherical behavioral zones

Results obtained with the traditional Spherical behavioral zones (figure 2.3) will be reviewed first. The school shapes and structures brought about by Spherical behavioral zones function as null-model for runs with differently shaped behavioral zones.

3.1.1 School shape

The schools of individuals with Spherical behavioral zones are oblong and become more oblong as the group size increases (table 3.1, figure 3.1). The width of the school is a bit larger than its height, which is presumably due to forces which inhibit vertical movement (equation 2.18). Standard deviation in school height (0.85) is therefore lower than school width (2.01).

Group size	School shape		
	L	W	H
50	6.29	4.53	4.50
250	16.0	7.50	7.36
750	30.4	10.7	9.76
1500	45.0	13.7	11.2

Table 3.1: Average School Length Width and Height during 9 runs with Spherical behavioral zones

In general, simulation studies of schooling provide little data or explanations why certain school shapes emerge. We analyze the direction in which the sum of the separation and cohesion force is most active to understand the emergence of the shape of the school. The separation and cohesion force facilitate respectively the repulsion and attraction among individuals and thus influence the space between the individuals and therefore the shape of the school. The sum of the separation and cohesion force, which from now on will be called *spacing force*, is used because these forces usually work in opposite directions (figure 3.2).

The alignment force is not included in the spacing force as it is of less importance with respect to the shape of the school. The alignment force namely merely adjusts the heading of the agent to that of its neighbors and does not give rise to acceleration or deceleration, which

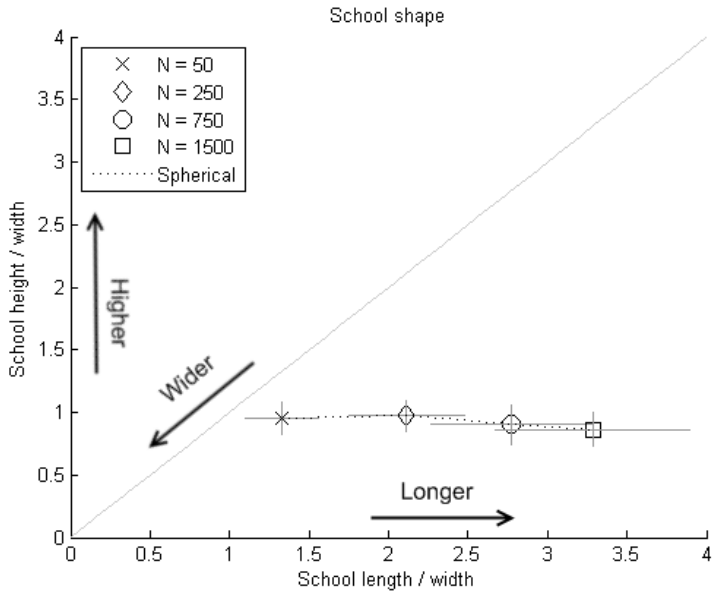

Figure 3.1: Relative school length, width and height for runs with Spherical behavioral zones. The different markers indicate different group sizes (see legend). The gray bars coming from the markers indicate the standard deviation. Larger group sizes bring about more oblong schools.

is an important factor in the emergence of the shape of the school according to Hemelrijk and Hildenbrandt [23]. Furthermore, the direction of the alignment force does not change with the shape of the behavioral zone. The alignment force is only active in lateral directions (figure 3.2), making it disadvantageous to be incorporated in the spacing forces as it would obscure differences between the distributions.

The distributions of the spacing forces contain the sum of the separation and cohesion forces for each agent during one run. The spacing forces of individuals with Spherical behavioral zones are most active towards the rear (figure 3.3a). This means that agents with Spherical behavioral zones are most likely to decelerate as a result of the interaction with their neighbors, which explains the oblong schools. This supports the forementioned explanations made by Hemelrijk and Hildenbrandt [23] and indicates that the spacing forces distribution is an useful tool to understand school shape.

Why do Spherical behavioral zones mainly cause deceleration? Firstly, the agents cannot drift left or right, but have to change their heading before they can move in another direction. This causes agents to accelerate or decelerate more often rather than change their orientation. Secondly, an agent cannot perceive neighbors in its blind angle, which means that an agent will decelerate as a response to close-by neighbors in front, but not accelerate when agents swim behind him.

3.1.2 Bearing and elevation angles

In runs with Spherical behavioral zones the nearest neighbors are more frequently found in front and at the rear of individuals than in lateral positions (figure 3.4a). There seems to be a

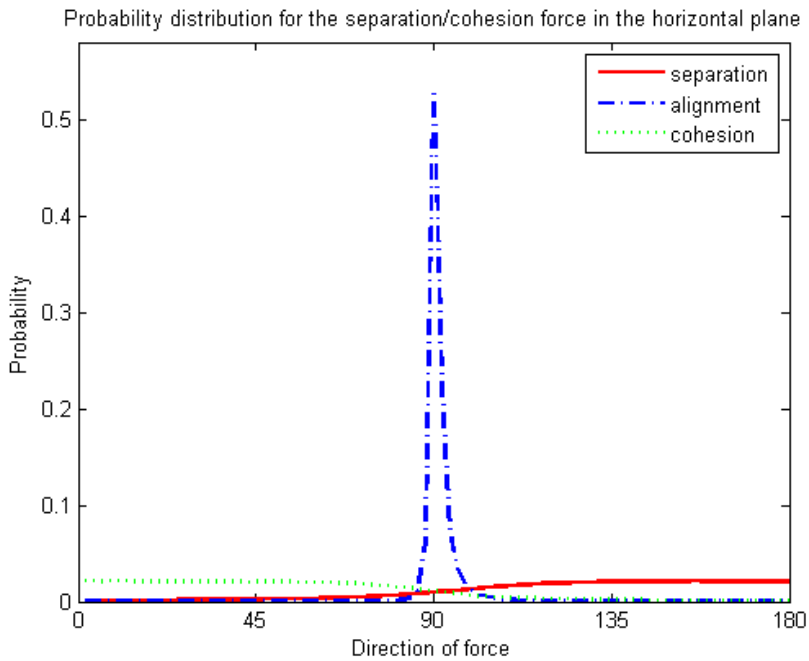

Figure 3.2: The probability distribution of the directions of the separation, alignment and cohesion forces in the horizontal plane. The direction of the force indicate the angle of the force in reference to the heading of the agent.

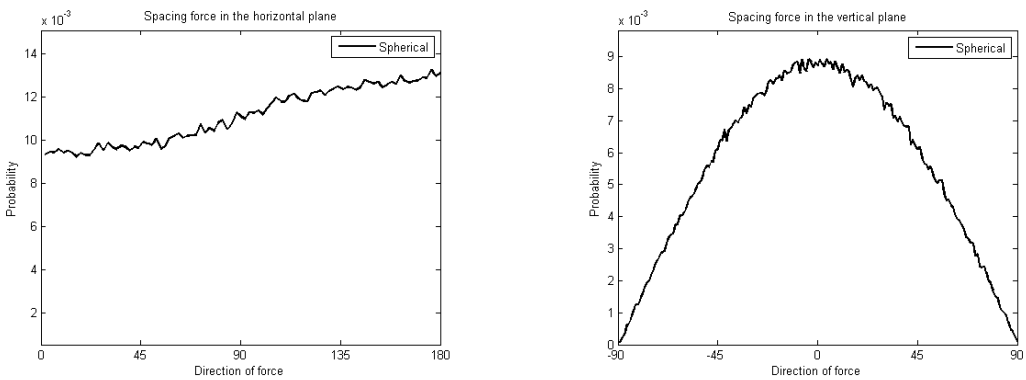

(a) Forces in the horizontal plane

(b) Forces in the vertical plane

Figure 3.3: The probability distribution of the combined separation and cohesion forces in the horizontal (a) and vertical (b) plane for a run with 1500 individuals with spherical behavioral zones. The direction of the force indicate the angle of the force in reference to the heading of the agent.

preference to swim in the blind angle of other agents. The individuals have a blind angle of 45 degrees (table 2.1), which corresponds to the increase in frequency in bearing angles between $0° - 45°$ and $135° - 180°$. Furthermore, the individuals' nearest neighbors are most often found swimming at the same depth (figure 3.4*b*).

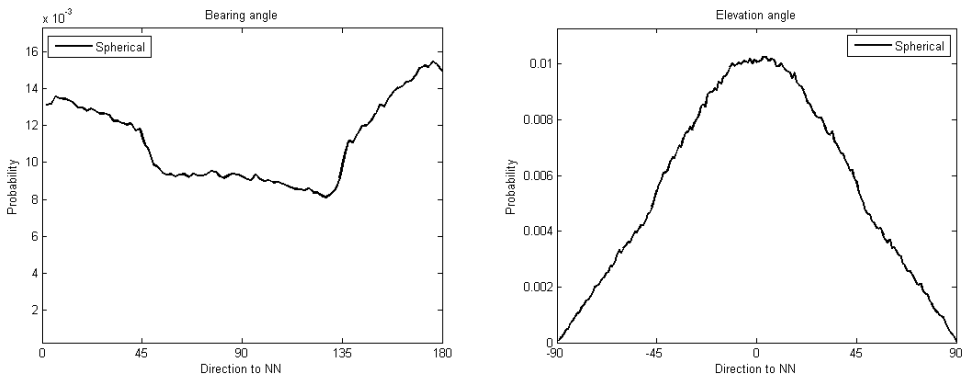

(a) Bearing angle ***(b)*** Elevation angle

Figure 3.4: The angle to the nearest neighbor in the horizontal (a) and vertical (b) plane.

3.1.3 Measurements in the vertical plane

Measurements of the spacing forces in the vertical plane (figure 3.3*b* and 3.8*b*,*d* and *f*) and the elevation angle (figure 3.4*b* and 3.14*b*,*d* and *f*) show typical distributions with zero probability at angles of 90° and −90°. This is caused by the presence of a Jacobian factor in the transformation from Cartesian to spherical coordinates [10]. This bias can be illustrated with an example: take a sphere uniformly filled with points. The sphere will have many more points on the equator than on the poles, despite the uniform distribution of points. The same bias causes the probability distributions of the elevation angle and spacing forces in the vertical plane to be zero at angles of −90° and 90°. Huth showed an alternative method to measure the elevation angle which adjusts for the aforementioned bias [28]. The elevation angles in the present study are not corrected for this bias because all empirical measurements of the elevation angle in fish schools are neither. Furthermore, deviations in the spacing forces in the vertical plane and elevation angle can easily be investigated because the distributions are all compared to the null-model case, Spherical behavioral zones.

3.2 Influence of shape of the behavioral zones

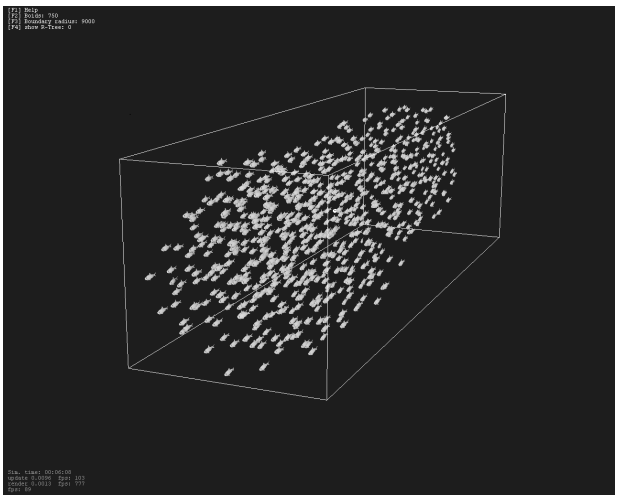

(a) Spherical behavioral zones

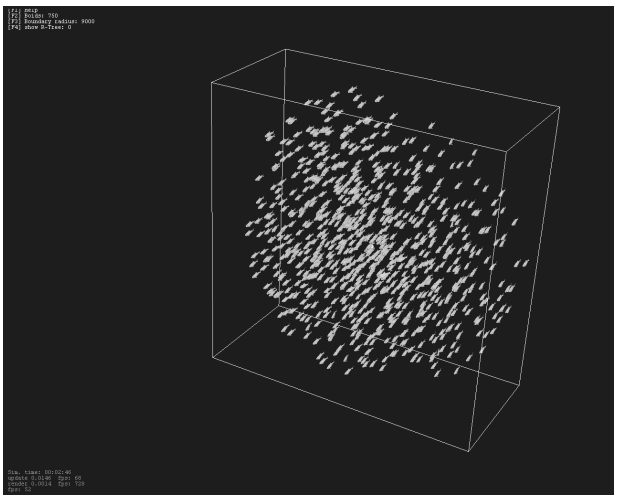

(b) Short behavioral zones

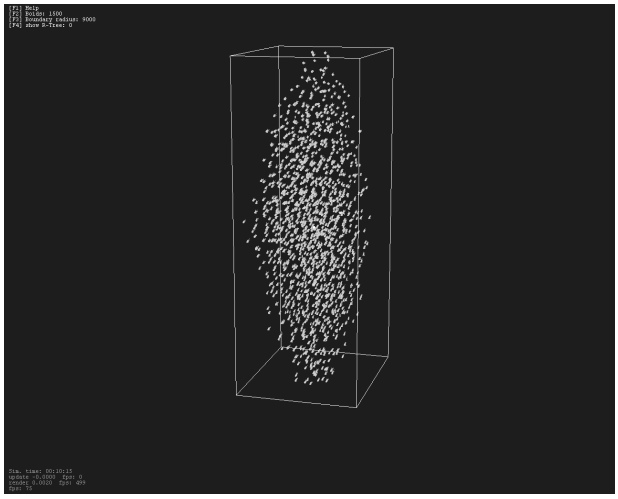

(c) High behavioral zones

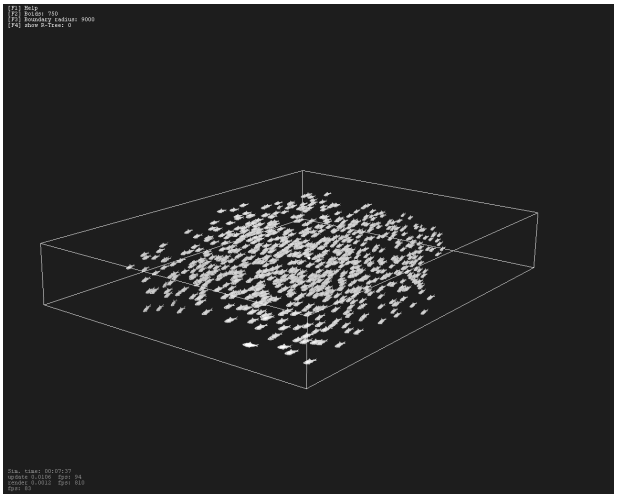

(d) Flat behavioral zones

Figure 3.5: Screen shots of runs with a group size of 750 and Spherical, Short, High and Flat behavioral zones. All the schools swim towards the bottom left of the figure. There is a clear relation between the shape of the behavioral zones and school shape.

3.2.1 Emerging school shapes

The shape of behavioral zones has a clear influence on school shape. The schools generally adopt, or exaggerate, the shape of the behavioral zones. Short, High, Flat, Wide, Narrow and Long behavioral zones bring about school shapes that could therefore be described as short, high, flat, wide, narrow and long (table 3.2 and figures 3.5 and 3.6).

The emerging school shapes do not always perfectly reflect the shape of the behavioral zones. Agents that have Flat behavioral zones, just as with Spherical behavioral zones, have a

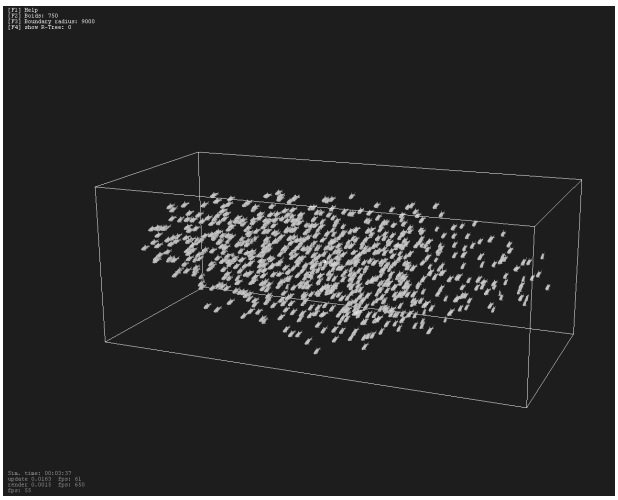

(a) Wide behavioral zones

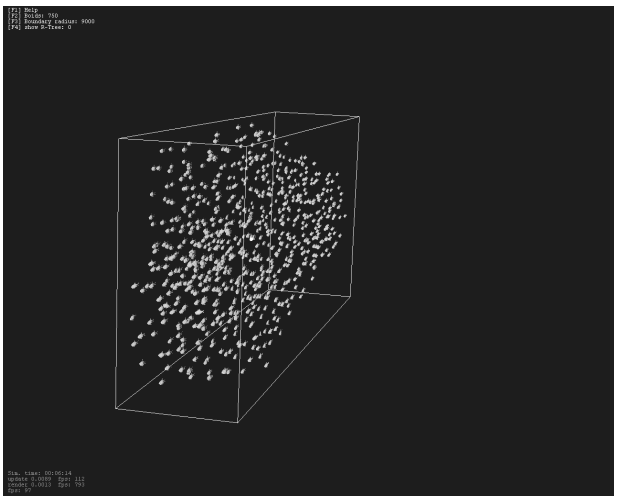

(b) Narrow behavioral zones

(c) Long behavioral zones (school type I)

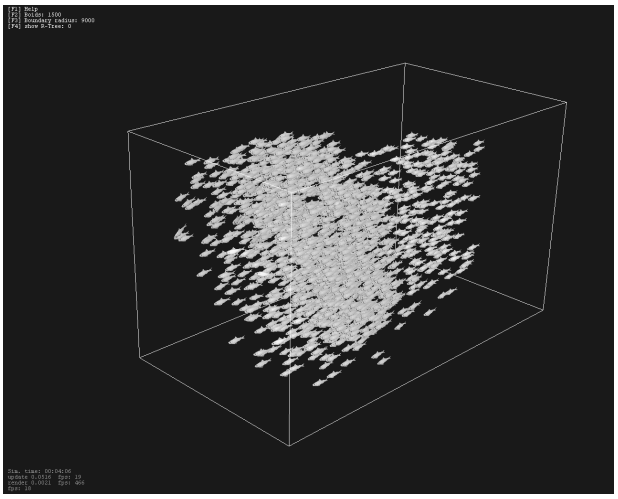

(d) Long behavioral zones (school type II)

Figure 3.6: Screen shots of runs with Wide, Narrow and Long behavioral zones. (a) and (b) are runs with a group size of 750. (c) and (d) are runs with a group size of 1500. Two plots (c and d) are displayed of runs with Long behavioral zones, because two different school formation were observed. All the schools swim towards the bottom left of the figure.

tendency to decelerate as a result from interacting with their neighbors. The schools brought about by Flat behavioral zones are therefore not only flat but also oblong (table 3.2).

If school shape would precisely reflect the shape of the behavioral zones, Long and Narrow behavioral zones would give rise to more oblong schools than Spherical behavioral zones. This, however, is only the case when the schools contain 50 and 250 individuals. With group sizes of 750 and 1500, Long and Narrow behavioral zones bring about relatively less oblong schools compared to schools brought about by Spherical behavioral zones (figure 3.7).

Group Size	50	250	750	1500
	L : W : H	L : W : H	L : W : H	L : W : H
Sphere	6.12 : 4.66 : 4.40	15.7 : 7.55 : 7.25	29.8 : 11.0 : 9.66	43.0 : 13.4 : 11.3
Wide	4.78 : 5.89 : 3.79	8.20 : 13.9 : 6.30	10.9 : 22.8 : 8.64	13.0 : 31.2 : 10.3
Narrow	7.39 : 3.86 : 4.26	16.5 : 6.96 : 7.64	24.2 : 9.92 : 12.2	27.5 : 11.0 : 16.7
High	4.70 : 3.94 : 6.06	8.30 : 6.19 : 13.9	11.1 : 8.82 : 22.4	13.4 : 10.7 : 30.2
Flat	8.56 : 6.03 : 2.16	17.5 : 11.5 : 2.91	30.2 : 19.8 : 3.89	42.4 : 28.4 : 4.25
Long	9.45 : 4.50 : 3.3349	20.0 : 7.83 : 5.22	21.8 : 9.88 : 7.80	23.4 : 12.0 : 11.0
Short	4.01 : 5.06 : 5.40	6.40 : 11.0 : 11.1	8.17 : 16.9 : 16.9	9.31 : 22.0 : 22.0

Table 3.2: Average absolute length, width and height of the school for all differently shaped behavioral zones.

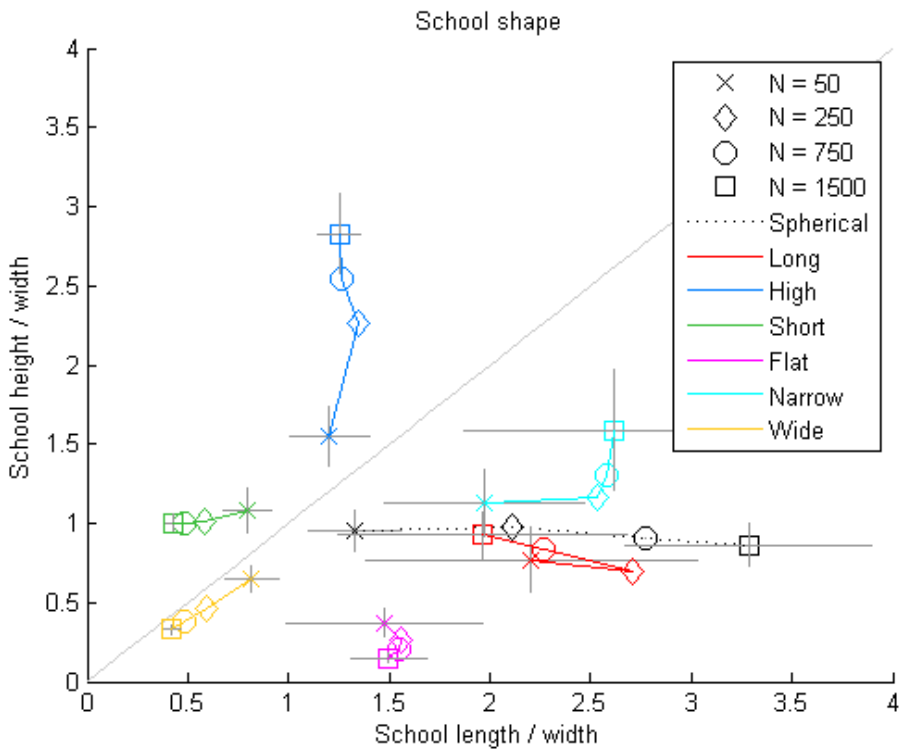

Figure 3.7: Relative school dimensions for all shapes of behavioral zones and group sizes. All shapes of behavioral zones, except Long behavioral zones, give rise to schools which become more asymmetric with group size. The error bars indicate the standard deviation. The standard deviation is only plotted for group sizes of 50 and 1500 to keep the graph readable. The standard error of the mean is not used here as it is smaller than 0.01 for all shapes.

3.2.2 Explaining school shape

The spacing forces are used to explain the emergence of the observed school shapes. The spacing forces during runs with Spherical behavioral zones are most active towards the rear,

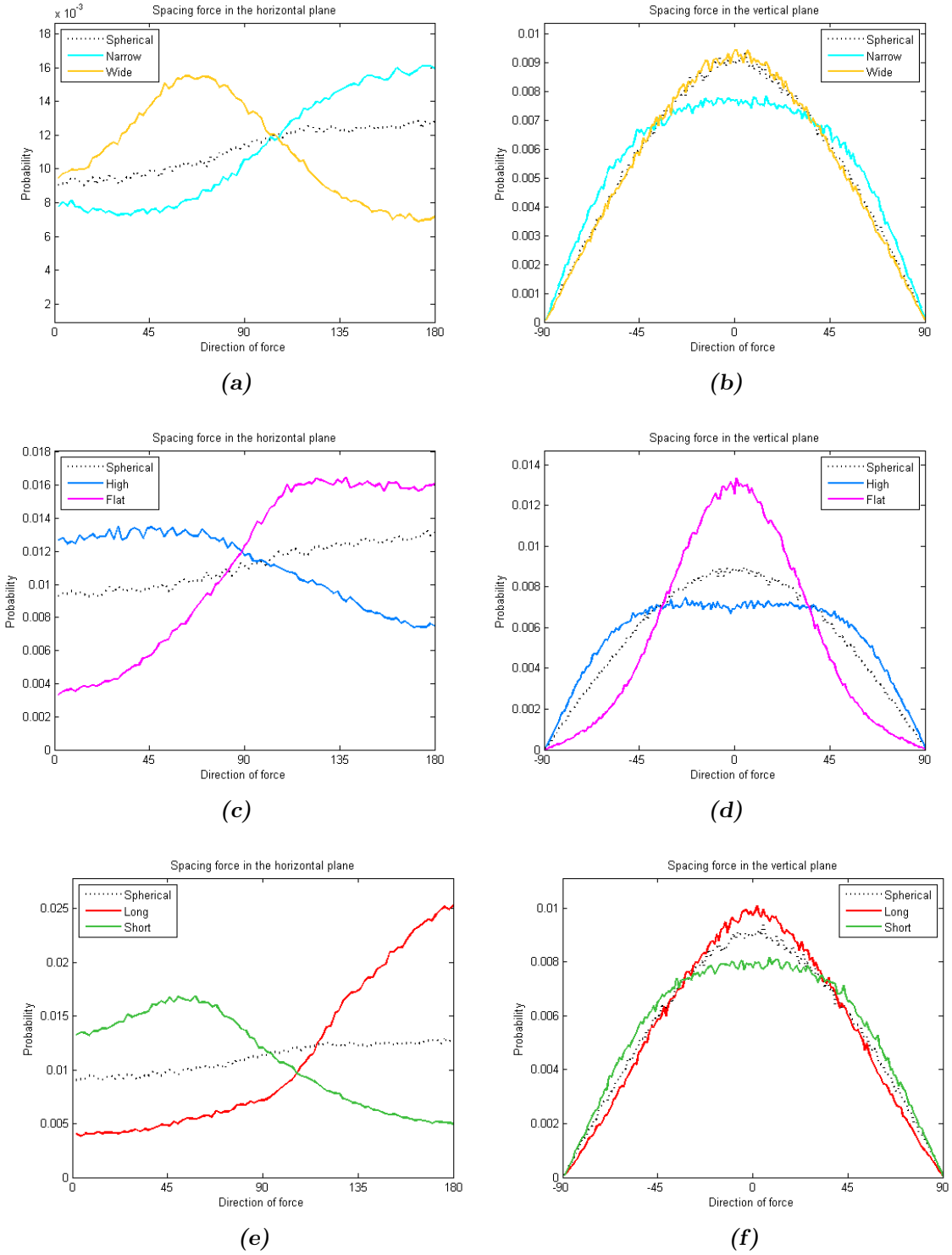

Figure 3.8: Spacing forces measured for schools induced by all differently shaped behavioral zones in the horizontal and vertical plane. The spacing forces of the runs with Spherical behavioral zones are plotted in each graph as a reference.

which indicate that agents decelerate more often as a result of interacting with their neighbor, explaining the oblong school shape. The distribution of the spacing forces during runs with

non-spherical shapes of behavioral zones resemble the observed school shapes as well. High behavioral zones, for example, induce spacing forces which work most often up- and downwards (figure 3.8*d*), corresponding to the high schools (figure 3.5*c*).

The relative direction of the neighbors with respect to the focal agent determines in which direction a behavioral response is executed. Thus, changing the shape of a behavioral zone means changing the volume that induces a behavioral response in a certain direction (figure 3.9).

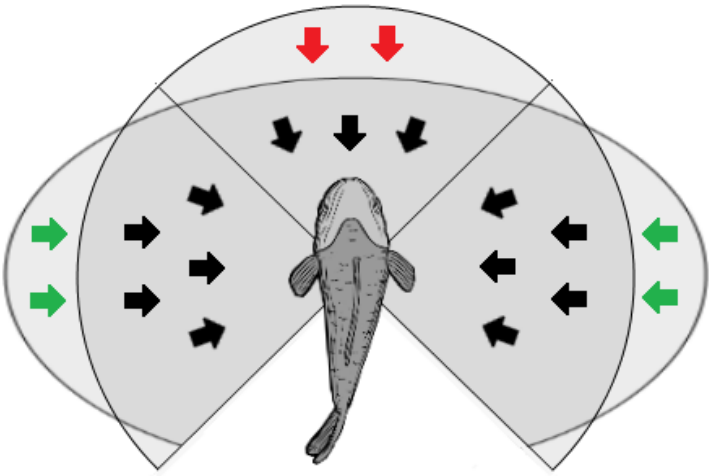

Figure 3.9: A Wide separation zone superimposed on a Spherical separation zone. The arrows roughly indicate the direction of the separation force to an agent at that position. The *green* arrows indicate the separation forces that are only present when a Wide separation zone is used and the *red* arrows indicate the forces that are only present when the separation zone is spherical. Changing the shape of the separation zone from Spherical to Wide results in a larger part of the behavioral zone that induces lateral movements and a smaller part that give rise to deceleration.

With Wide behavioral zones an agent more often perceives neighbors at its side than in other directions. The spacing forces in runs with Wide behavioral zones are therefore more active in the lateral directions (figure 3.8*a*). Whenever an individual has more neighbors on one side of its separation zone, the separation force will be directed to the other side. The center of the school is more dense than the periphery (Appendix figure A.3*c*). Agents to the left or right of the core are pushed towards the periphery because the number of neighbors in the separation zone is bigger on one side of the core than on the other. This creates a temporary gap which causes more individuals to have an unequal number of neighbors on each side. And thus leads to more steering away from the core of the school, widening the school even further. The temporary gap could also be filled by agents swimming just behind the gap, making the school shorter and thus relatively wider.

The mechanism which causes High behavioral zones to give rise to high school shapes is similar to the one described for the emergence of a wide school shape. The proportion of the volume of the separation zone which creates up and down movements is larger than the volume which produces movements into the other directions. The center of a school is denser than the periphery (Appendix figure A.3). Agents swimming above or below it thus have more agents on the center side of the school, reinforcing the agents to move further up or down. The

spacing forces are therefore more frequently directed up- or downwards compared to Spherical and especially the Flat zones (figure 3.8*d*).

The spacing forces in runs with Flat behavioral zones are predominately horizontal and directed towards side and the rear of the individuals (figure 3.8 *c* and *d*). This indicates that the individuals are pushed away from the core of the school, mainly towards the side and rear, thus making the school flat. The blind angle at the rear causes individuals to have a bias towards deceleration instead of lateral movement because the individuals do not observe the agents behind them making the flat schools longer than they are wide.

The schools brought about by all shapes of behavioral zones have a bias towards deceleration instead of vertical or horizontal movements. The schools are therefore a bit more elongated than the shape of the behavioral zones (see table 3.2 at the beginning of this chapter).

Short behavioral zones are not only short but also high and wide (figure 2.9), when compared to Spherical behavioral zones. Individuals with Short behavioral zones experience less spacing forces directed backwards and more in the lateral and vertical directions (figure 3.8 *e* and *f*) as the proportion of the separation zone which produces this behavior is bigger. The individuals are pushed away from the core into the vertical or lateral direction, making the school high and wide.

As group sizes increase almost all schools gradually become more asymmetric. Usually the most striking feature of the school shape becomes more prominent as larger group sizes are used. For example wide schools become even wider with larger group sizes (figure 3.7). Runs with Narrow and Long behavioral zones show a different pattern; here a clear switch in school shape between the runs with different group sizes can be observed.

First the emergence of the school shape induced by Narrow behavioral zones will be discussed. Schools with 50 or 250 individuals with Narrow behavioral zones are oblong and more oblong than schools brought about by Spherical behavioral zones. Narrow behavioral zones are more elongated than Spherical ones, what means agents react earlier to others in front of them. This causes agents to decelerate more, which leads to a more oblong school. Schools consisting of 250 individuals with Narrow behavioral zones are on average more elongated than the schools of 50 individuals (figure 3.7), meaning the school length increases in relation to the school width. The schools with group sizes of 750 or 1500, however, are not much more elongated but mainly higher than the schools of 50 and 250 individuals. The packing densities increase with larger group sizes (figure 3.17). Higher densities coincide with smaller distances between agents. Agents cannot avoid close-by agents by only decelerating when the inter-individual distances are very small. The agents therefore often end up laterally or vertically besides a neighbor which was previously swimming in front. Agents swimming above each other are repulsed further upwards, more so than lateral neighbors are repulsed sideways as the (Narrow) behavioral zones are higher than they are wide (figure 2.7). This happens more often with higher densities and thus makes the school shape relatively higher when group size is increased (figure 3.7).

Schools with individuals that have Long behavioral zones do not get more asymmetric when larger group sizes are used. Schools containing 250 individuals with Long behavioral zones are more elongated than schools with 50 individuals. However, for group sizes of 750 and 1500 the schools are less elongated (figure 3.7). During runs with group sizes of 750 and 1500 multiple school shapes are observed. The schools are very elongated (figure 3.6 *c*) or a lot less elongated

and contain one or several slices with densely packed agents throughout the width of the school (figure 3.6 *c* and *d*). The slices remain constant over time, as the shape and size usually do not change for the remainder of the run once a slice has formed. This phenomenon is more often observed in schools with large group sizes, which is why schools with 1500 agents are on average less elongated than schools with fewer individuals.

Why do these patterns emerge with larger group sizes? Larger group sizes bring about larger packing densities (figure 3.17), and thus smaller distances between the agents. The Long behavioral zones differ from the Narrow zones in the sense that the width of the Long zones is equal to the height (figure 2.8). This allows the agents to be positioned, not only close together laterally similar to runs with Narrow zones, but also vertically. Additionally, once the individuals are inside the forementioned slice, the shape of the zones allows the agents to keep swimming together because there is not much lateral nor up- or downwards repulsion.

The packing densities for runs with Long behavioral zones are not only a lot higher than in runs with any other shape, but additionally show much larger deviations (figure 3.17). The dense slices do not arise every run, which explains the larger deviations in packing density and nearest neighbor distance (figure 3.16). To further show the influence of local density on the emergence of different school types, the relation between the elongation of the school for individuals with Long behavioral zones and the cohesion weights, which affects local density, is investigated.

3.2.3 Influence of local density on school shape

A phase transition is found in schools brought about by individuals with Long behavioral zones. As mentioned in the previous section, dense slices of agents form within the school when group sizes of 750 and higher are used. This phenomenon is presumably caused by the increase in packing density which arises due to the larger group sizes. In this section the influence of density on school shape and structure is further investigated. The cohesion weight is varied, instead of the group size, to obtain schools with different levels of density in runs with Long behavioral zones. Higher cohesion weights give rise to larger attraction forces between the agents and thus induces denser schools (figure 3.11a).

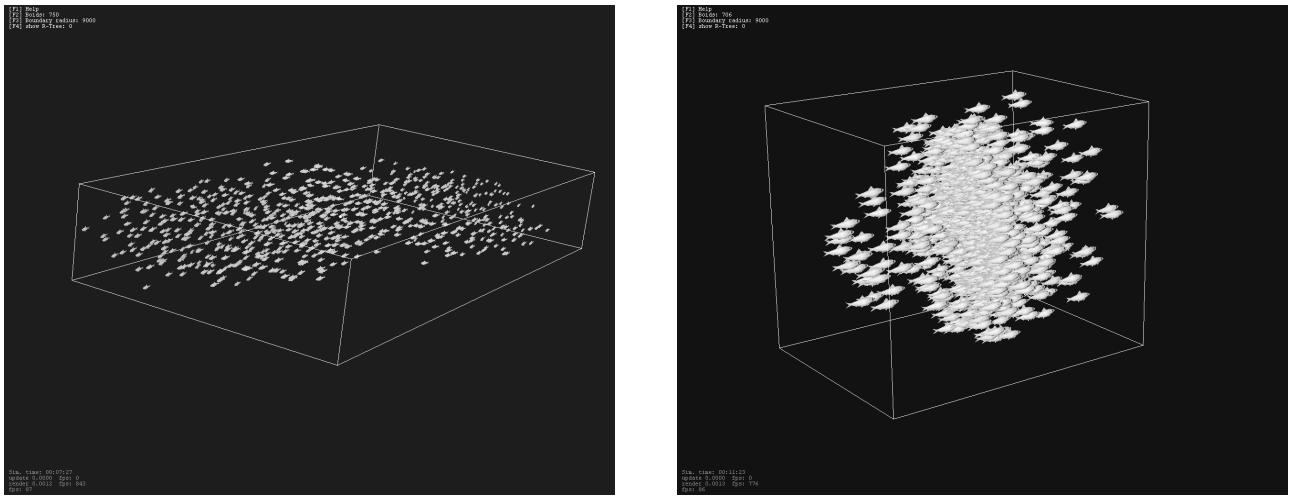

(a) Cohesion weight: 7 $BL^2\,BM/s^2$ ***(b)*** Cohesion weight: 11 $BL^2\,BM/s^2$

Figure 3.10: Screenshots taken of schools with individuals possessing Long behavioral zones using different cohesion weights. Larger cohesion weights bring about higher densities, which cause the agents to form schools with dense slices rather than an oblong school. (a) Loose aggregated oblong school swimming towards the bottom-left. (b) Densely packed school swimming towards the upper-right.

Dense slices of agents emerge in runs with Long behavioral zones and high cohesion weights (figure 3.10), even more clearly than they did with regular cohesion weights and group size of 750 and 1500. This verifies that the phase transition, found with a regular cohesion weight in schools induced by Long behavioral zones, is the result of higher densities brought about by larger group sizes. The increase in density causes school brought about by Long behavioral zones with 1500 individuals to be less oblong than schools with less individuals (figure 3.7). Higher cohesion weights to bring about similar patterns, i.e. the schools get less oblong when higher cohesion weights are used (figure 3.11b).

The phase transition in school shape can be found by increasing group size or by increasing cohesion weights, as both give rise to higher densities. Higher packing densities correspond to smaller distances between the agents. This causes agents more often to steer to the side rather than decelerate to avoid and thus more often end up next to each other. The long shape of the behavioral zones facilitates this as the agents are not repulsed backwards once they swim next to each other. The spacing forces indicate that for higher cohesion weights the agents are

pressed together and not repulsed backwards (figure 3.12).

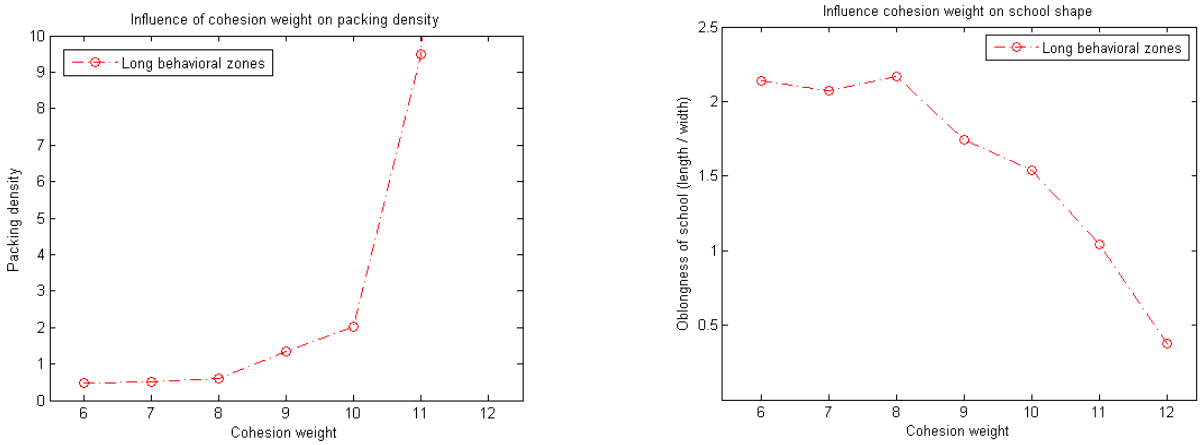

(a) ***(b)***

Figure 3.11: (a) Larger cohesion weights bring about higher packing densities. (b) Larger cohesion weights bring about less oblong schools, i.e. the school length-width ratio becomes smaller.

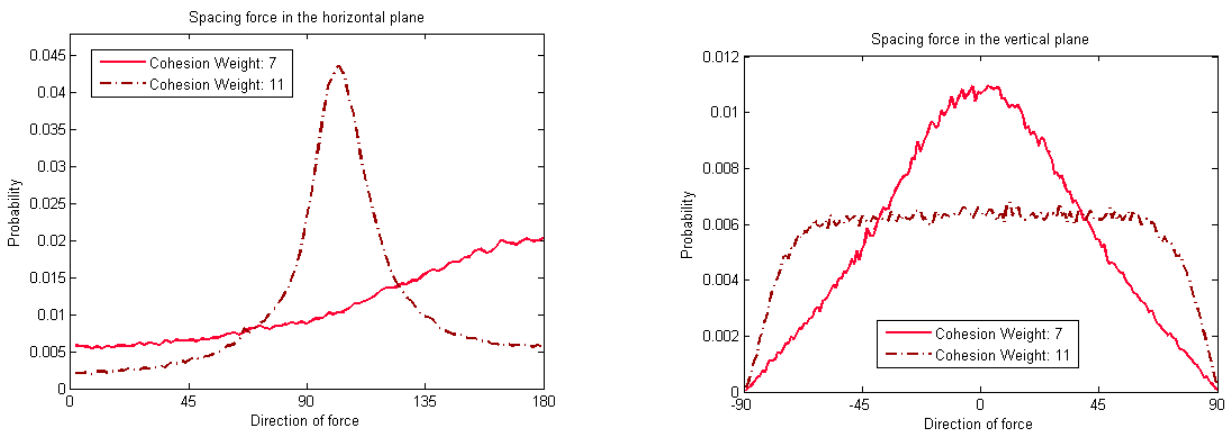

(a) ***(b)***

Figure 3.12: Spacing forces in the horizontal (a) and vertical (b) plane for runs with Long behavioral zones and cohesion weight 7 and 11 $BL^2\,BM/s^2$. Individuals avoid each other through deceleration when a cohesion weight of 7 $BL^2\,BM/s^2$ is used. Higher cohesion weights bring about spacing forces which are more often side-, up- and downwards.

Influence cohesion forces on bearing angle

Besides an influence on packing density and thus on school shape, the strength of the cohesion weights also has an interesting effect on the probability distribution of the angle towards the nearest neighbor in the horizontal plane, i.e. the bearing angle. Individuals with Long behavioral zones, when the cohesion weight is smaller than 9 $BL^2\,BM/s^2$, have their nearest neighbor more often at lateral bearings than in front or at the rear (figure 3.13).

The nearest neighbors are less frequently found at lateral bearings and more often found in the blind angle (at bearings between 135° and 180°) when the cohesion weights increase (figure 3.13). These results are interesting because during the experiments to find the influence of differently shaped behavioral zones bearing and elevation angles (which we will discuss later on), we did not encounter schools of agents with preferred bearing angles at 90°. These findings indicate that we can lower the cohesion weights to increase the influence of the shape of the behavioral zones and neutralize the bias in agents to swim in the blind zone of other agents.

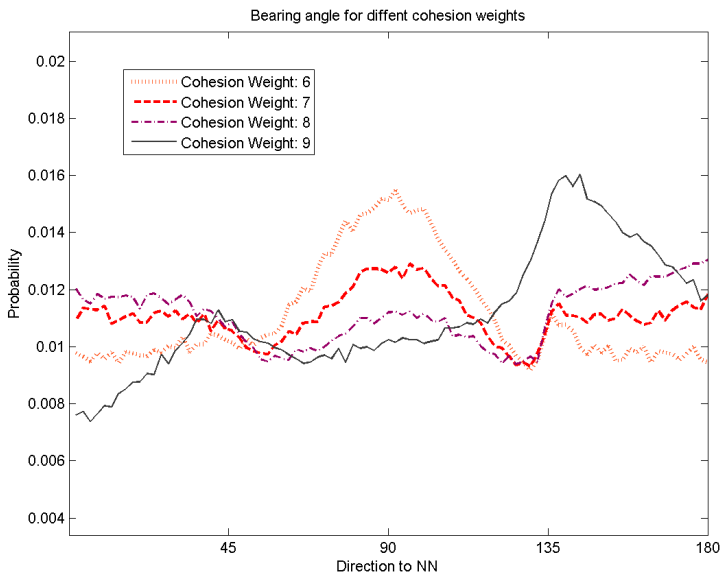

Figure 3.13: The nearest neighbors are more often found in lateral positions (at a bearing angle of 90°) when cohesion weights lower than 9 $BL^2\,BM/s^2$ is used. For higher cohesion weights (9 $BL^2\,BM/s^2$ and higher), the nearest neighbors are more often found at the edge of the blind angle, thus at a bearing of 135°. The bearing angles of runs with cohesion weights 10 to 12 are not plotted because they are very similar to the bearing angles found in runs with a cohesion weight of 9 $BL^2\,BM/s^2$.

3.2.4 Bearing and elevation angles

The shape of the behavioral zones does not only influence the shape but also the structure of the school. The global density, nearest neighbor distance, bearing and elevation angle do all change with the shape of the behavioral zones. The influence of differently shaped behavioral zones on the angle towards the nearest neighbor in the horizontal plane (bearing angle) and in the vertical plane (elevation angle) will be discussed.

The magnitude of the blind angle strongly influences the positioning of the individuals within the school. The most frequent angles with which the agents swim in relation to their nearest neighbor are $0° - 45°$ or $135° - 180°$ (figure 3.14). This means that agents swim often within the blind angle of neighboring agents. This arises because agents do not perceive others in their blind angle and are therefore not repulsed by them. Note that the 45° blind angle of the individuals correspond to the most frequently found bearing angles. Similar patterns are found in a model of schooling fish by Hemelrijk and Hildenbrandt [24]. The authors show, for multiple blind angles, that the bearing angle of most nearest neighbors adopts the blind angle of individuals.

A notable difference between the various bearing angle distribution is that the bearing angles found in runs with Flat and Long behavioral zones have more agents on the edge of their blind angle (figure 3.14*c* and *e*). This is partially caused by collision avoidance behavior, which steers individuals to the edge of the blind angle when preceding agents come to close. This phenomenon is only visible when individuals possess Long or Flat behavioral zones seeing that these individuals tend to brake the most (figure 3.8*c* and *e*).

Interestingly, the shape of behavioral zones seems to have little effect on the bearing angle distributions, besides aforementioned small differences obtained with Long and Flat behavioral zones. Intuitively you would expect that the nearest neighbors are located where they experience the least amount of separation, thus where the radius of the separation zone is smallest. For example, in runs with Narrow behavioral zones you would expect to see a large proportion of the neighbors to be found at bearings of 90°. However, the difference between the bearing angle of Narrow and Wide behavioral zones is almost non-existing (figure 3.14*a*), while these two shapes are very different (especially in the horizontal plane) and create very different school shapes.

The elevation angle is more affected by the shape of the behavioral zone than the bearing angle, as the differences between the distributions of differently shaped zones are more substantial (figure 3.14 *b,d* and *f*). Spherical and Wide behavioral zones bring about schools where the nearest neighbors are most frequently found on the same depth (figure 3.14 *b*). On the other hand, in runs with Long and especially Flat behavioral zones the nearest neighbors are more frequently on different depths (figure 3.14 *d* and *f*). Individuals with Flat behavioral zones are predominately repelled by individuals on the same horizontal plane, more so than individuals with other shapes of behavioral zones. Individuals swimming at a different height are thus more often the nearest neighbor as they are not repulsed away.

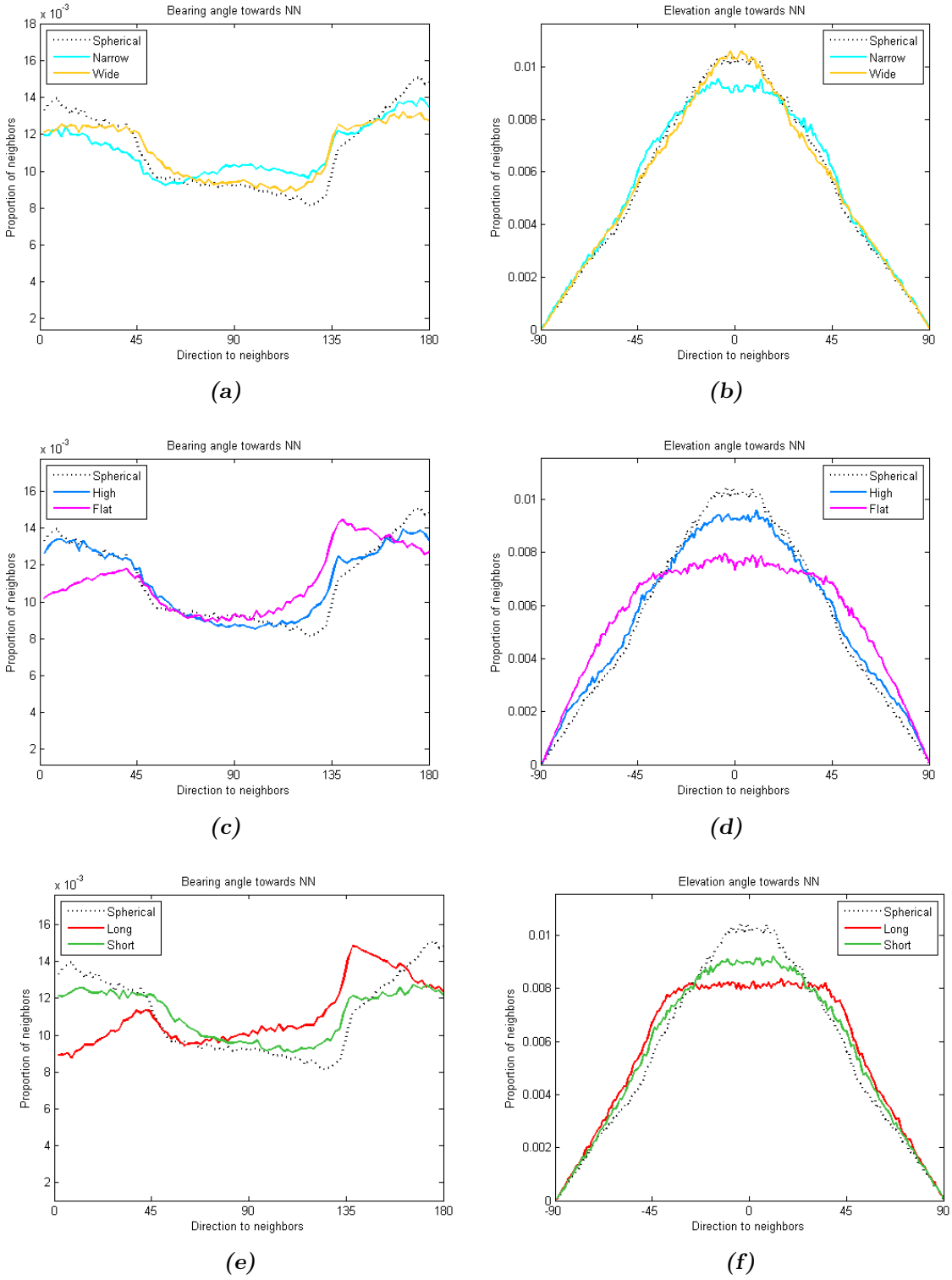

Figure 3.14: The bearing angle (a,c and e) and elevation angle distributions (b,d and f) for all the differently shaped behavioral zones. The bearing and elevation angle of the runs with Spherical behavioral zones are plotted in each graph as a reference. A bearing angle of 0° corresponds to a nearest neighbor located to the front and 180° to the rear. An elevation angle of −90° corresponds to a nearest neighbor located directly below, and 90° to above. The shape of the behavioral zones seem to have little effect on the bearing angle distribution.

3.2.5 Bearing and elevation angles with a low cohesion weight

A previous section showed that as the cohesion weight is reduced, the nearest neighbors of agents with Long behavioral zones have a lower tendency to swim in a blind angle (figure 3.13) and are more often found at lateral positions. This indicates the small influence of the shapes of the behavioral zones on the bearing angles could be due to the bias to swim in the blind angle. This section shows the effects of reducing the cohesion weight from the regular 9 $BL^2\,BM/s^2$ to 7 $BL^2\,BM/s^2$ on the distributions of the bearing and elevation angles.

A reduced cohesion weight makes the individuals have a lower tendency to swim in the blind angle of other agents, while the influence of the shape of behavioral zones consequently becomes more apparent (figure 3.15). The bearing angles distributions brought about with a lower cohesion weights are more intuitive on account of the nearest neighbors that are now more often found at positions where the radii of the separation zone is smallest, thus where they experiences the least amount of repulsion.

The nearest neighbors are most frequently found at lateral positions when the individuals use Narrow behavioral zones, whereas with Wide behavioral zones the nearest neighbors are more often in front or at the rear (figure 3.15a). The distributions of the bearing angles found with Narrow and Wide behavioral zones are now each others opposite, while the distributions of the bearing angles are similar when we use a cohesion weight of 9 $BL^2\,BM/s^2$ (figure 3.14 a). The bearing angles of Long and Short behavioral zones also differ notably when a lower cohesion weight is used, while they hardly differed with a cohesion weight of 9 $BL^2\,BM/s^2$. Long behavioral zones bring about school structures where the nearest neighbors are more often at lateral positions, whereas Short behavioral zones induce individuals to swim directly in front of or behind their nearest neighbors (figure 3.15 e).

The distributions of the bearing angles for High and Flat behavioral zones does not change much when a lower cohesion weight is used. This is because the shapes of the High and Flat behavioral zones in the horizontal plane are identical, i.e. the length of the radii of the zones do differ but they have the same length-width ratio (figures 2.4 and 2.5). Obviously, High and Flat zones differ in the vertical plane, hence the distribution of the *elevation* angle do too. The elevation angle of runs with Flat behavioral zones is the only elevation angle which shows a bimodal distribution (figure 3.15d). The separation zone has a larger influence when the cohesion weight is lowered. The neighbors on the same movement plain around an individual are therefore more effectively repelled away. Hence neighbors swimming at different depths will even more often become the nearest neighbor. The opposite takes place for individuals with High behavioral zones. Neighbors just above or below an individual are repulsed away more than agents swimming at the same depth, which explains why the nearest neighbors are more often found around elevation angles of 0° (figure 3.15d).

In general it is thus found that flatter zones bring about more often spatial structures where the nearest neighbors are more often found at different depths, and higher zones cause nearest neighbors to be more often found on the same depth. Long and Wide behavioral zones are relatively flat when comparing their respective length and width with the height of both behavioral zones (table 2.2). Consequently, both elevation angles show more nearest neighbors at different heights compared to runs with Spherical behavioral zones.

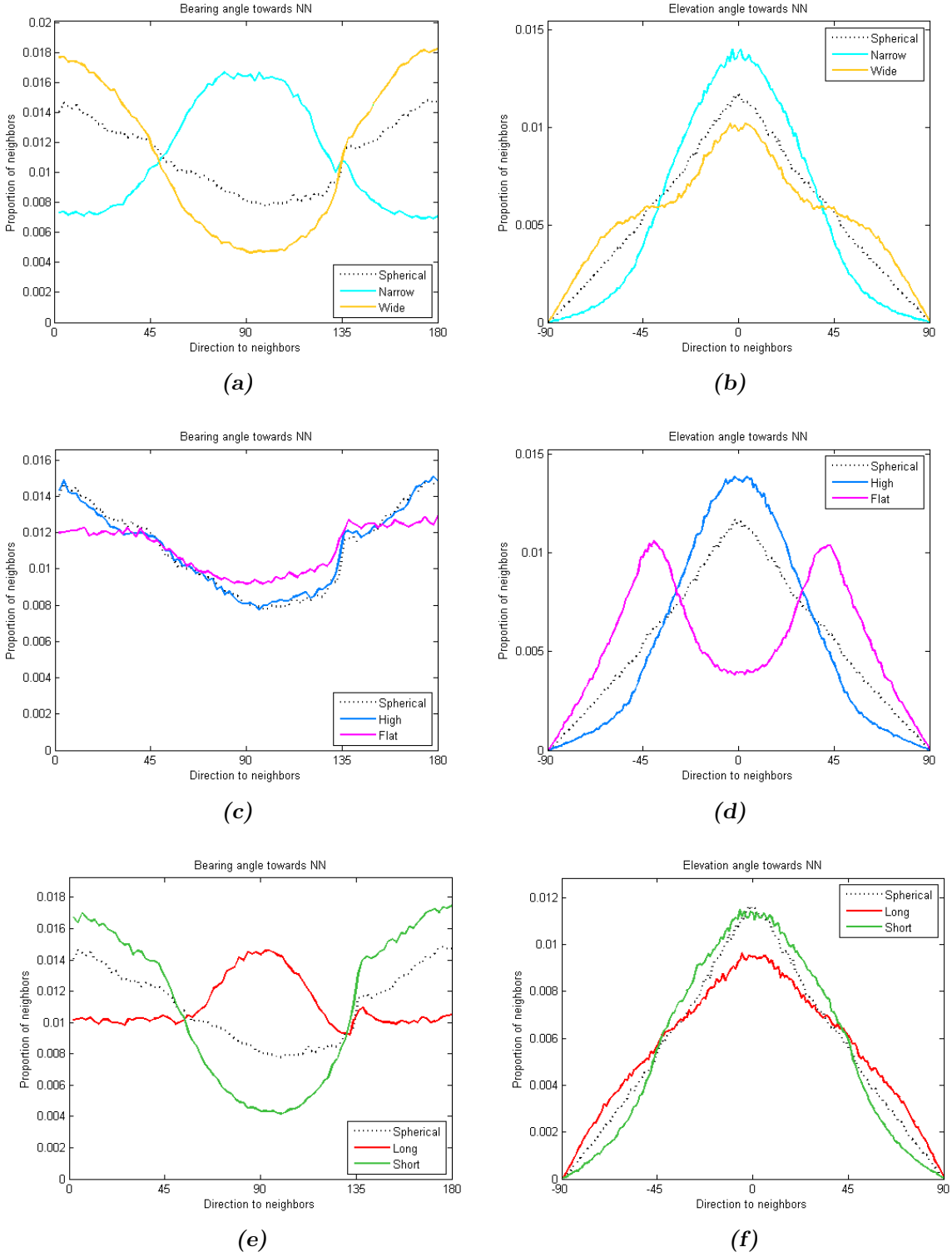

Figure 3.15: The bearing angle (a,c and e) and elevation angle (b,d and f) distributions for all different shapes of behavioral zones with a (lowered) cohesion weight of 7 $BL^2\,BM/s^2$. With a lowered cohesion weight, the bearing and elevation angle distributions show large variations due to different shapes of behavioral zones. A bearing angle of 0° corresponds to a nearest neighbor located to the front and 180° to the rear. An elevation angle of −90° corresponds to a nearest neighbor located directly below, and 90° to above.

3.2.6 Density

Another aspect of the school structure is the nearest neighbor distance (NND) and packing density. Spherical behavioral zones bring about the highest nearest neighbors distances and the lowest packing densities (figure 3.16 and 3.17). Non-spherical behavioral zones have a separation zone which is in some directions smaller than the spherical one. This allows the nearest neighbors to get closer and cause the school volume to decrease and packing densities to increase. The nearest neighbor distance and packing density are both significantly negatively correlated with group size for all the various shapes of behavioral zones (Appendix table A.2 and A.3). The influence of group size on packing density and NND is smallest for Spherical behavioral zones and biggest for Long behavioral zones. Long behavioral zones give rise to the highest deviations in NND and packing density, which can be explained by the emergence of multiple school types in runs with group sizes of 750 and 1500 (figure 3.6*c* and *d*).

The shapes of behavioral zones which bring about the smallest NND, also brings about the highest packing densities, with the exception of runs with Flat behavioral zones and a group size of 1500 (figure 3.16). The NND measured in runs with Flat behavioral zones are (for any group size) a lot smaller compared to the NND in runs with other shapes, while the schools brought about by Flat behavioral zones are not much denser than the other shapes of behavioral zones. This could mean that packing density is less affected by asymmetry in behavioral zones than NND is, considering Flat behavioral zones zones are more asymmetric than other shapes (table 2.2). Or, the relative low packing densities in runs with Flat behavioral zones could be caused by a bias in the voxel-based volume calculations (section 2.3.2). Schools brought about by Flat behavioral zones are, compared to other schools, more asymmetric and therefore have a relatively high percentage of neighbors at the periphery of the school (Appendix table A.4). Relatively more neighbors at the periphery corresponds to a higher surface-to-volume ratio which means that the voxel-based school volume measurements suffer more from overestimation due to the 'edge-effect' (section 2.3.2).

An increase in packing density and decrease in NND does not necessarily mean that all the individuals swim closer to each other [10]. Schools with larger group sizes have a lower surface-to-volume ratio, and thus have a lower percentage of individuals swimming on the periphery of the school and higher percentage of inner individuals (Appendix table A.4). Schools with 50 individuals have 30 to 40% individuals located inside the school, while schools with 1500 individuals have 60 to 75% (Appendix table A.4). Individuals inside the school are more densely packed in comparison to individuals on the periphery (figure 3.18), which causes higher packing densities and lower nearest neighbor distances to be measured in schools with larger group sizes.

Cavagna et al. suggest omitting individuals at the periphery to avoid the bias in different surface-to-volume ratios when performing density measurements [10]. Omitting individuals at the periphery from the density measurements does not bring about very different results (Appendix figure A.5) compared to the results discussed earlier in this section. Furthermore, the surface-to-volume ratio of a school is caused by the school shape which is a side-effect of the shape of the behavioral zones. All the individuals of the school should therefore be taken into account when performing density measurements, despite of the bias due to different surface-to-volume ratios.

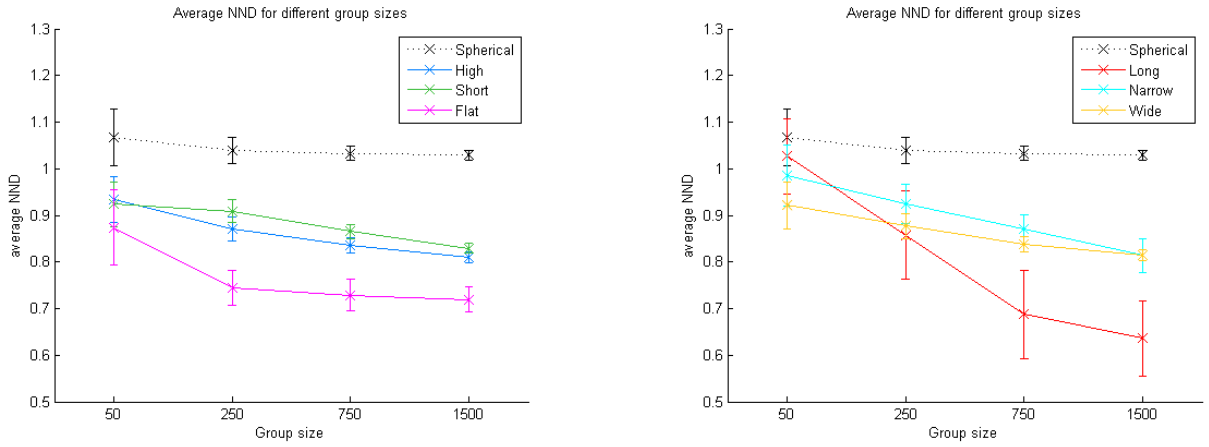

(a) ***(b)***

Figure 3.16: The average nearest neighbor distance (NND) for all shapes of behavioral zones per group size. The NND becomes smaller with group size. Schools brought about by Long behavioral zones show the largest decrease in NND, whereas schools induced by Spherical behavioral zones shows the smallest decrease.

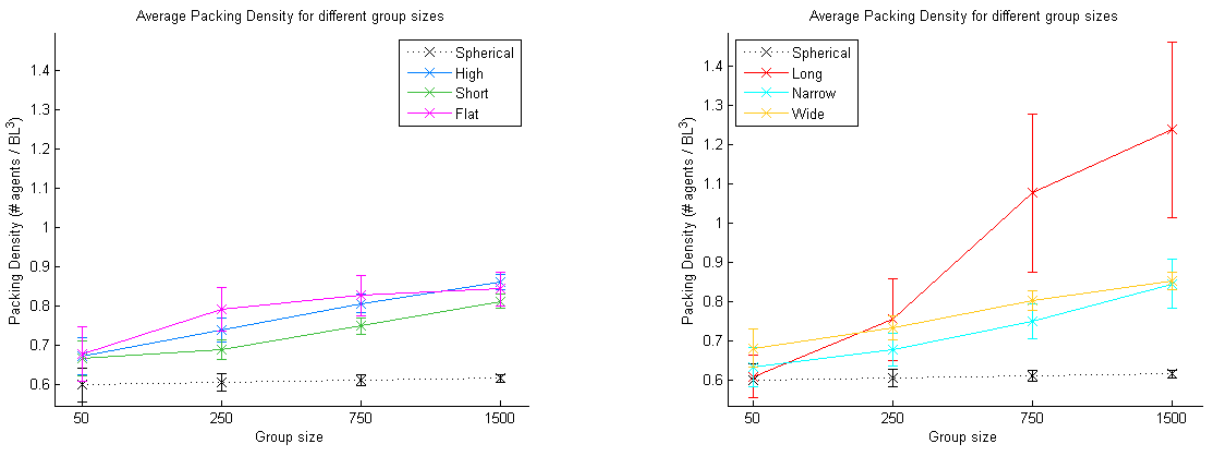

(a) ***(b)***

Figure 3.17: The average packing density for all shapes of behavioral zones per group size. The packing density increases with group size. Schools brought about by Long behavioral zones show the largest increase in packing density, whereas schools induced by Spherical behavioral zones shows the smallest increase.

3.2.7 School speed

The individuals have a desired cruise speed of 2.5 $BL\ sec^{-1}$, but the real swimming speed varies due to interactions with conspecifics. The shape of the behavioral zones facilitate the interaction with conspecifics, and thus affect the average speed of the individuals in the school, i.e. the school speed (figure 3.19).

The length of the separation zone is negatively correlated (Kendall tau = -0.8197, n = 63,

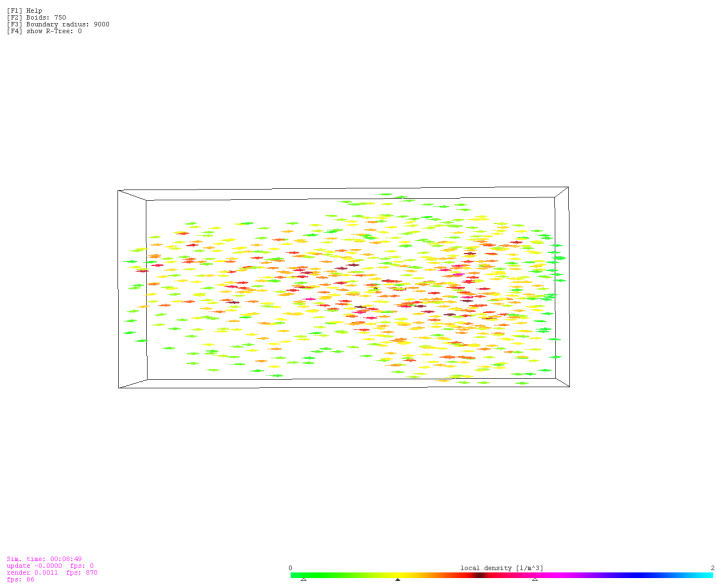

Figure 3.18: A top-down view of a school with 750 individuals that have Spherical behavioral zones. The colors of the agents indicate the local density as experienced by the individuals. The density inside the school is higher than at the pheriphery. Appendix figure A.3 shows the local density plots of schools with individuals using the other shapes of behavioral zones.

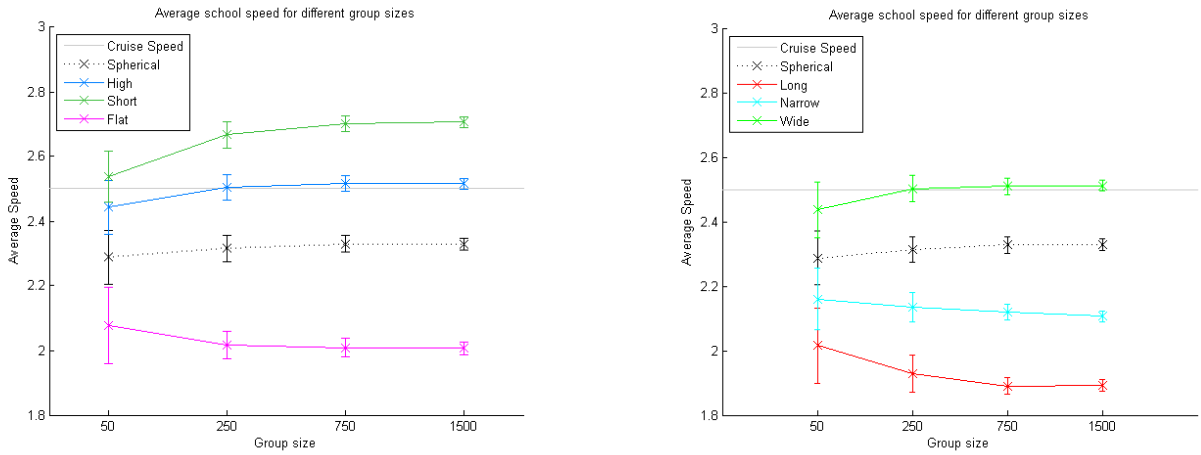

(a) ***(b)***

Figure 3.19: Average school speed for runs with differently shaped behavioral zones. The gray straight line signifies the desired cruise speed of the agents. Short, High and Wide behavioral zones bring about school speeds that faster the preferred cruising speed of the individuals. See text for explanation.

$p < 0.001$) with the average speed of the school (table 3.3). Longer behavioral zones, and thus longer separation zones, make the individuals react sooner to individuals in front of them. This reaction more often brings about deceleration since the part of the separation zone which induces deceleration compared to lateral or vertical movements is relatively large for longer separation zones. Runs with Flat behavioral zones give rise to faster school speeds than Long

behavioral zones, even though the radii of the Flat behavioral zones are a bit more extended in the traveling direction (table 3.3). This is because Long behavioral zones bring about denser schools than Flat behavioral zones (figure 3.17). Agents with Long behavioral zones therefore decelerate more often and thus give rise to slower school speeds.

Shape	School speed	Length separation zone
Short	2.71	1.25
High	2.51	1.35
Wide	2.51	1.35
Spherical	2.33	1.50
Narrow	2.11	1.66
Flat	2.01	1.93
Long	1.89	1.92

Table 3.3: Average School Speed over 9 runs for all shapes of behavioral zones with a group size of 1500. Longer separation zones give rise to slower school speeds.

Oblong schools (brought about by Spherical, Narrow, Flat or Long behavioral zones) are slower than shorter schools (brought about by Short, High, Wide behavioral zones). Empirical studies show similar patterns, namely that faster schools of saithe are less oblong than slower schools [39]. Hemelrijk and Hildenbrandt also found that faster schools are less oblong by varying the preferred cruise speed ($2.0\,BL\,sec^{-1}$ to $4.0\,BL\,sec^{-1}$) of individuals [23]. Our results resemble those found by Kunz and Hemelrijk since they also show that longer behavioral zones bring about slower schools, i.e. elliptical behavioral zones bring about slower schools than circular behavior zones [**?**]. Their results differ from ours in the sense that elliptical agents in their model bring about wide schools. Hence their wide schools are slower than their oblong schools, were we find the opposite.

As mentioned before, the blind angle is mainly responsible for the tendency to decelerate because agents can perceive neighbors in front of them but not behind them. Most shapes of behavioral zones have therefore an average school speed below the preferred cruise speed of the individuals. Short, Wide and High behavioral zones, however, have an average school speed above the preferred cruise speed, regardless of the blind angle at the rear.

How can the school speed become higher than the preferred cruising speed of the individuals? Short, Wide and High behavioral zones induce spacing forces which are more active to the front, $0° - 90°$, than to the rear, $90° - 180°$ (figure 3.8*a,c* and *e*). The individuals thus more often accelerate rather than decelerate as a result of the interactions with their neighbors. Short, Wide and High behavioral zones give rise to schools which are relatively short in relation to their height and/or width. This decreases the amount of deceleration because most agents swim next to rather than behind each other. Additionally, these school shapes have a relative large percentage of agents swimming at the front periphery of the school compared to oblong schools. Individuals at the frontal periphery are occasionally propelled out in front of school, due to neighbors at the edge of the blind angle of the separation zone. A very low local density is perceived by the individuals when they have sped out in front of the school, what causes their behavioral zones (and thus separation zones) to grow (due to equation 2.15). The school speed becomes larger than the preferred cruising speed of the individuals due to this difference in size of the behavioral zones, because the individuals which are still in the school have smaller

separation zones and will mainly be attracted (and not repulsed) towards the individuals who sped out in front of the school.

The propulsion of agents and the attraction by the rest of the school which causes the school speed to be above the preferred cruise speed of the individuals resembles mechanisms found in novel studies of migrating locust [4, 44]. Collective motion of locusts is partially driven by cannibalistic motivations, i.e. the desire to eat other locust who are ahead and the fear of getting eaten by conspecifics from the rear. Interestingly, we get our results with individuals which have a blind angle at the rear, whereas locusts can detect conspecifics behind them [4].

3.3 Empirical observations

Schools with individuals that have Spherical behavioral zones, are oblong and become more oblong as group size increases (table 3.1). These results correspond to the findings of Hemelrijk and Hildenbrandt [23]. Similar patterns are found in empirical studies, larger schools of herring were observed to be more elliptical than smaller schools [2]. Empirical data do not only show that fish schools are oblong but also that the width of the schools is in most species larger than the height. The 'Length : Width : Height' ratio of schools of pilchard is observed to be 2.1 : 1.7 : 1.0 [16], 3 : 2 : 1 in minnows [41], 4 : 2 : 1 in mullets [7], 2 : 4 : 1 to 10 : 4 : 1 in cod, 6 : 3 : 1 in saithe and 3 : 3 : 1 in herring [39, 42]. Even though there are many different species which show different school shapes, the height is in all cases smaller than the width. The schools in the present model with individual possessing Spherical, Long and Narrow behavioral zones all give rise to oblong schools, but the height of the school is not significantly smaller than the width. Flat behavioral zones, however, bring about (relative) school shapes which range from 4.0 : 2.8 : 1.0 for schools of 50 individuals to 10 : 6.7 : 1 for schools of 1500 individuals and thus resemble school shapes observed in real fish.

Empirical measurements of bearing and elevation angle vary much per species although general patterns can be extracted. Empirical observations of bearing angles show consistently two different distributions: firstly, bearing angles which show a bimodal distribution with peaks at ranges of 30° - 70° and 130° - 160° like in schools of herring and saithe (figure 3.20c) and to some degree in bluefin tuna (figure 3.20b). And secondly, unimodal distributions of bearing angles with most nearest neighbors at a bearing of 90°, thus at lateral positions, like in schools of pollocks (figure 3.20a) and cod (figure 3.20c). Furthermore, all the bearing angle distributions of real fish school show that the nearest neighbors do not often swim directly in front of or behind other fish. Most fish produce a vortex wake by undulating with a strong backwards component. As it is not hydrodynamically advantageous for fish to swim within this wake, nearest neighbors are presumably found less often at bearings of 0° and 180°.

All the bearing and elevation distributions found in empirical studies can be observed in the present model. The bearing angles for various different shapes of behavioral zones with the cohesion weight 9 $BL^2\,BM/s^2$, show a bimodal bearing angle distribution. Long and Flat behavioral zones bring about schools that best resemble real schools, because they both (like in empirical data) have a small proportion of nearest neighbors found directly in front of or behind them (figure 3.21 a). The high densities in runs with Long and Flat behavioral cause the collision avoidance behavior to become active and steer the individuals towards the edge

of blind angle. A lower cohesion weight, 7 $BL^2\,BM/s^2$, gives rise to lower densities. Long and Flat behavioral zones remain to bring about bimodal bearing angles distribution, but with a higher proportion of neighbors at bearings of 0° and 180° (figure 3.21 a), because the collision behavior becomes less often active.

Besides bimodal bearing angles, empirical measurements show unimodal bearing angle distributions (figure 3.20a and c). This means that the nearest neighbors are most often found in lateral positions. Long and Narrow behavioral zones, as they both have a separation zones which are more long than wide, give rise to unimodal bearing angles when a cohesion weight of 7 $BL^2\,BM/s^2$ is used (figure 3.22a).

The elevation angle distributions in empirical data vary per species as well. The nearest neighbors in herring and saithe schools are more often found at a different depth, indicated by a bimodal elevation angle distribution and thus a small proportion of nearest neighbors at an elevation of 0°. Cod on the other hand has its nearest neighbor more often swimming at the same depth (figure 3.20 d) [39]. In the model most shapes of behavioral zones bring about a school structure with most nearest neighbors swimming at the same depth, thus an unimodal elevation angle with a peak at 0°. Only in runs with Flat behavioral zones and a low cohesion weight are the nearest neighbors more often at a different depth, illustrate by the bimodal distribution of the elevation angle with peaks at 45° and −45° (figure 3.21b).

Which shape of behavioral zones gives rise to the most natural schools? Flat behavioral zones induce school shapes, bearing angle and elevation angles that resemble empirical measurements. Irregardless of the weight of the cohesion behavior, Flat behavioral zones bring about schools which are flat and oblong, like real fish schools (table 1.1 in the introduction chapter). Furthermore, with a low cohesion weight (7 $BL^2\,BM/s^2$) Flat behavioral zones give rise to bimodal bearing angles and bimodal elevation angles (figure 3.21), which are similar to bearing angles *and* elevation angles found in tuna, saithe and herring (figures 3.20b,c and d). Using a cohesion weight of 9 $BL^2\,BM/s^2$, Flat behavioral zones produce natural bearing angles, but less natural elevation angles (figure 3.21).

The two types of bearing angle distributions found in empirical data, uni- and bimodal, suggest that there is not one shape of behavioral zones that can produce the behavior of all fish species. Unimodal bearing angle distributions, as observed in empirical studies of pollocks and cod (figure 3.20a and c), are observed in runs with Long and Narrow behavioral zones. However, school shapes and elevations angles measured in these runs do not match the empirical data. A new shape of behavioral zones, of which the length is greater than the width and the width is greater than the height, could presumably give rise to flat oblong schools with unimodal bearing angles and bimodal elevation angle distributions.

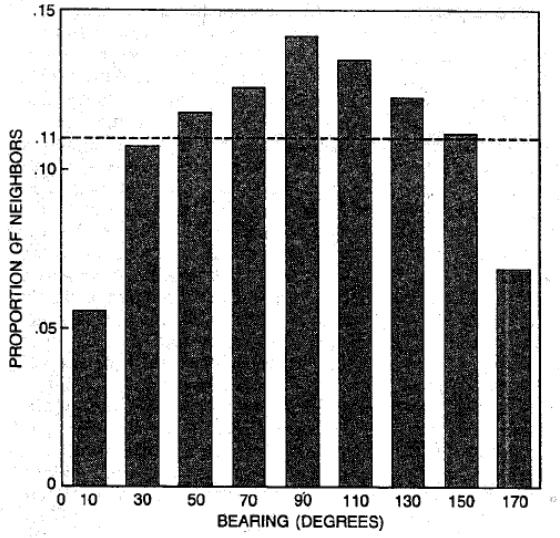

(a) Bearing angles in pollocks

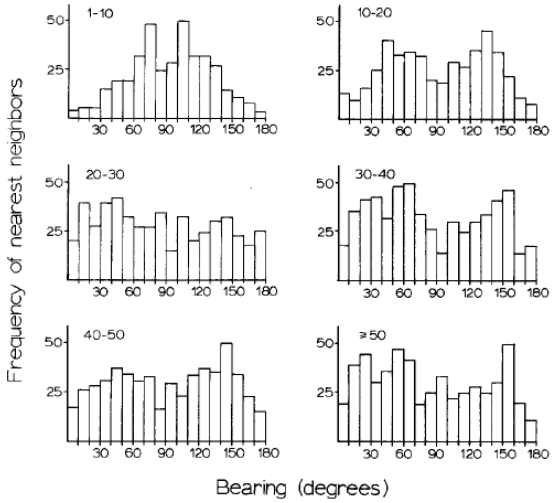

(b) Bearing angles in bluefin tuna

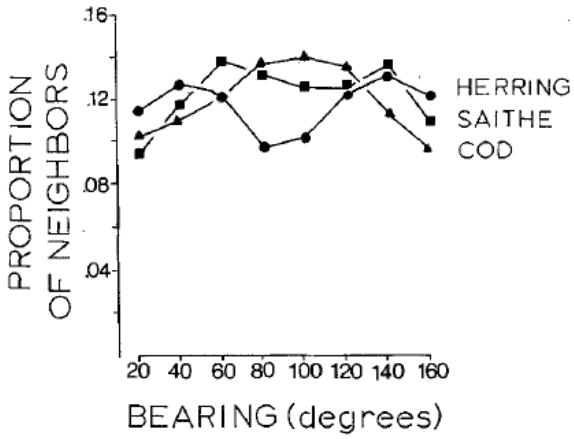

(c) Bearing angles in Saithe, Herring and Cod

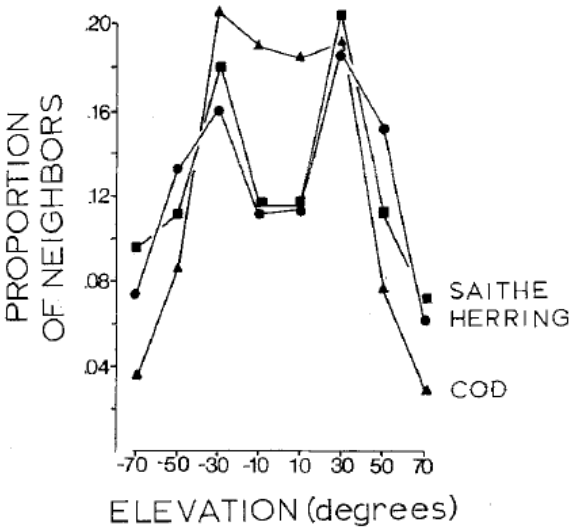

(d) Elevation angle in Saithe, Herring and Cod

Figure 3.20: Empirical data of the bearing and elevation angles. Empirical measurements show generally two different bearing angles distributions, unimodal distributions (like in pollocks *a* and cod *c*) or bimodal distributions (like in bluefin tuna *b*, saithe and herring *c*). Figures and data are originally published by (a) Partridge [37] (b) Partridge et al. [38]. (c and d) Partridge et al. [39]

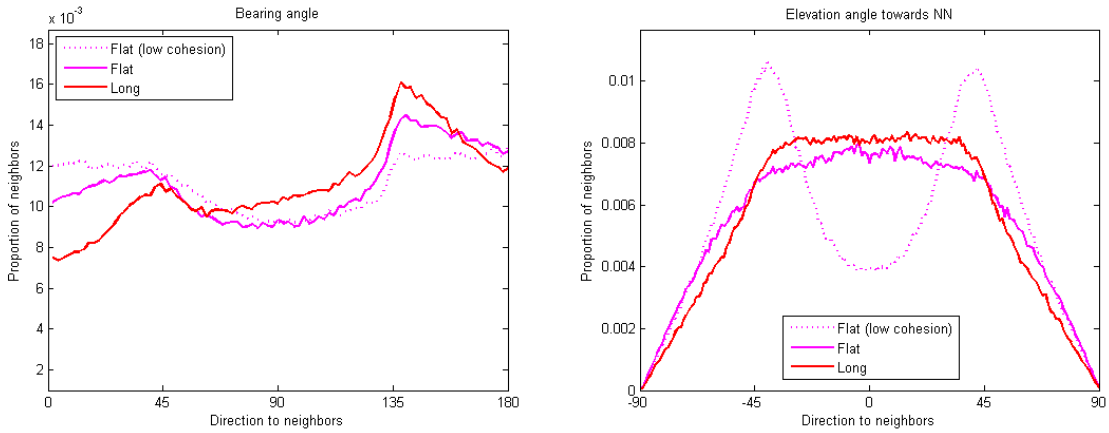

(a) Bearing angle ***(b)*** Elevation angle

Figure 3.21: The bearing angle and elevation angle of runs with Flat behavioral zones (low and regular cohesion weight) and Long behavioral zones. These distributions are used before in figures 3.14 and 3.15. a) Flat and Long behavioral zones bring about bimodal bearing angles distributions, similar to distributions found in bluefin tuna, saithe and herring (figures 3.20 *b* and *c*). b) Flat and Long behavioral zones both bring about school structures where the nearest neighbors are more often found on different depths. Flat behavioral zones with a lower cohesion weight bring about bimodal elevation angles distributions found in saithe and herring (figure 3.20*d*).

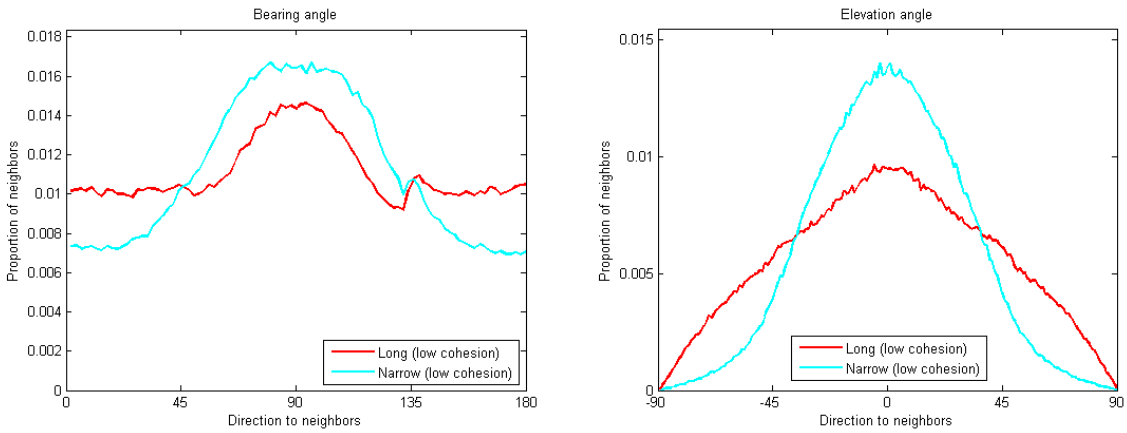

(a) Bearing angle ***(b)*** Elevation angle

Figure 3.22: The bearing angle and elevation angle of runs with Long and Narrow behavioral zones with lower cohesion weight). These distributions are used before in figures 3.14 and 3.15. a) Long and Narrow behavioral zones with a low cohesion weight bring about unimodal bearing angles distributions, similar to distributions found in cod and pollocks (figures 3.20 *a* and *c*). b) The elevation angles of Long and Narrow behavioral zones do not resemble elevation angles found in real fish.

Chapter 4

Discussion

This study shows the relation between the shape of behavioral zones and emerging school shape and structure. Measurements from runs with individuals that have the traditional Spherical behavioral zones were used as a null-model. The schools of individuals with Spherical behavioral zones were found to be oblong, similar to schools in research by Hemelrijk and Hildenbrandt [23], Hemelrijk and Kunz [25] and Kunz and Hemelrijk [34]. Hemelrijk and Hildenbrandt argue that the oblong school shape arises due to avoidance of other individuals by deceleration [23]. The present research provides evidence that supports this explanation. The most frequent direction of the spacing forces, i.e. the sum of the separation and cohesion force vectors, throughout a run with Spherical individuals is most frequently directed towards the rear of the individuals (figure 3.3). This shows that Spherical individuals are most likely to decelerate as a result of the interaction with other individuals, which causes the school to become (and stay) oblong.

This research further shows that a relative small change in the shape of the behavioral zones, i.e. the separation and alignment zone, has a big influence on school shape and structure. In general we can say that the shape of the behavioral zones is adopted and even exaggerated by the shape of the school. Schools of agents that have Flat, High, Short, Wide, Narrow and Long behavioral zones bring about flat, high, short, wide, narrow and long schools respectively. The shape of behavioral zones does not entirely describe the emerging school shapes. In most cases the schools are more oblong than the shape of the behavioral zones. This is due to the fact that the individuals are more likely to avoid others by decelerating than by changing their heading.

The clear relation between the distribution of the spacing forces (figure 3.8) and the observed school shapes show the effects of the shape of behavioral zones. Changing the shape of a behavioral zone means in effect changing the volume, or the frequency, with which the corresponding behavioral response is executed in a certain direction. School shape changes when a behavioral response is more often executed in one direction. Wide behavioral zones, for example, correspond to a relative larger volume (of the separation zone) which causes the agents to move laterally, resulting in a wider school.

The separation and cohesion responses are most influential with respect to the school shape, as these behaviors cause the individuals to steer away or towards the center of the school. The alignment behavior on the other hand has little influence on the school shape, as this behavioral response does not affect the inter-individual distances (directly) but merely adjusts

the orientation of the individuals.

It was found that a small change in the shape of the behavioral zones brings about a relative large change in the spatial organization of the school. The effects of the shape of behavioral zone is enlarged due to two reasons: firstly, the influence of the neighbors on the direction of the separation force is scaled along with the shape of the separation zone (equation 2.5), hence agents in a certain direction have a relative larger influence on the separation response. Secondly, the shape of the cohesion zone remained spherical for all the various shapes of the behavioral zones. The cohesion response predominantly operates in the opposite direction of the separation force (figure 3.2). Changing the cohesion zone along with the separation and alignment zone will therefore presumably lead to similar, but less extreme, school shapes.

Group size also affects school shape, as schools with more individuals give rise to more asymmetric school shapes, e.g. a wide school becomes wider and a flat school becomes flatter. Long behavioral zones are an exception to this trend. Schools with 750 or 1500 Long individuals are less oblong, and thus more symmetric, than schools with 50 or 250 individuals (figure 3.7). A phase transition takes place when group sizes become larger than 750 individuals (with Long behavioral zones). One or more densely packed slices of agents across the width of the school arise frequently with group size of 750 or more individuals (figure 3.6d). The frequency and the number of these slices per school increase when the group size grows. This explains why schools with more individuals get relatively less oblong for group sizes of 750 and 1500. The phase transition is the result of the increase in density which arise due to the larger group sizes. Experiments where the cohesion weight (w_c in equation 2.11) was varied to control the density of the school (figure 3.11a) confirm that these patterns arise due to an increase in density (figure 3.10).

Kunz and Hemelrijk performed experiments in a 2D model with behavioral zones that were either circular or elliptical [34]. The authors did not find a clear relation between shape of behavioral zones and school shape. Are group dynamics inherently different in 2D than in 3D? The present study shows that a deviation in the height of behavioral zones merely leads to change in the height of the school and the same goes for deviations in length and width. This implies that similar dynamics should work in a 2D model.

Agents in the model by Kunz and Hemelrijk swim at a fixed speed, which changes interaction patterns because the agents cannot slow down. The elliptical behavioral zones in their model therefore do not bring more deceleration but more lateral movements as they avoid frontal agents (sooner) by steering. The agents more often end up next to each other, creating a wider school instead of an oblong school. Note that the two-dimensional elliptical agents in the research of Kunz and Hemelrijk are the 2D version of the Long behavioral zones in the present study. Long behavioral zones in the present model generally do bring about oblong schools because these agents can decelerate, but with high packing densities schools with Long behavioral zones can become less oblong due to sideways avoidance just like in the model by Kunz and Hemelrijk.

The angle towards the nearest neighbor in the horizontal plane (bearing angle) and vertical plane (elevation angle) were used as a measure for school structure. Bearing and elevation angles are frequently used measurements in empirical studies of fish, but are rarely published for simulation studies of schooling fish. Huth is the only one who published bearing and elevation angles of his schooling agents [27]. The schools in Huth's model show a bearing angle with a near uniform distribution and unimodal elevation angle with a peak at 0°. These distributions

do not resemble bearing and elevation angles in real fish schools. Bearing angles in real fish schools are usually not uniform but show either a unimodal distribution with a peak at 90° or a bimodal distribution with peaks around 45° and 135° (figure 3.20*a* and *c*). Distributions of elevation angles in real fish schools show predominantly bimodal rather than unimodal (figure 3.20*d*). In the present model the nearest neighbors are most often located in the blind angle when a cohesion weight of 9 $BL^2\,BM/s^2$ is used. Lowering the cohesion weight causes the shape of the behavioral zones to have a large influence of the position of the nearest neighbors and thus on the distribution of the bearing and elevation angles.

Which shape of behavioral zones brings about schools that resemble the real fish schools best? Flat behavioral zones bring about schools that are flat and oblong and thus resemble schools of real fish (table 1.1). Flat behavioral zones additionally give rise to elevation angles also found in saithe and herring when a cohesion weight of 7 $BL^2\,BM/s^2$ is used. The bearing angles (when using the same cohesion weight) resemble the bearing angles of saithe and herring, although they do not match entirely because this model does not facilitate wake exploitation. The flatter school shape and bimodal elevation angles have never been observed in a model before and presumably can only emerge with behavioral zones that give rise to relatively less (separation) interactions among neighbors swimming at a different depth.

The shape and structure of real schools are influenced by many things: proximity of predators, currents, ocean surface or floor, and more. Flat oblong schools and bimodal elevation angles however are found in multiple fish species and different empirical studies, making it less likely that these patterns are merely caused by external influences as these conditions tend to vary per study. This study shows that these patterns can emerge from local interactions only. The good results obtained with Flat behavioral zones indicate that these interactions more often take place in the movement plane rather than the vertical plane.

What does this imply about real fish? Behavioral zones reflect the sensory capabilities *and* the behavioral responses of fish. The good fit of the schools brought about by Flat behavioral zones can therefore mean multiple things. Either the lateral line system of fish has difficulty sensing neighbors above or below them, or fish react less strongly to vertical neighbors.

Fish might pay less attention to vertical neighbors because their vortex wakes cannot be exploited. In addition, fish are inhibited to change depth [33], thus individuals do not have to pay much attention to neighboring agents above or below them to avoid any collisions.

It is difficult to determine the three-dimensional range of a lateral line system, as for example the level of sensitivity of the lateral line system is dynamic. Fish reduce through efferent signals the sensitivity of the hydrodynamic sensors to mask hydrodynamic waves induced by their own movement [6]. There are, however, some morphological indications that the lateral line system is less sensitive to vertical cues. For example, the hair-cells in the lateral canals that sense the hydrodynamic pressure waves are predominantly orientated in anterior or posterior directions and not in vertical (dorsal/ventral) directions [20, 46].

Ćurčić-Blake and van Netten show that a straight lateral line (1 dimensional) can accurately determine the position of vibrating source in a two-dimensional field [17], but presumably not in a three-dimensional field. This implies that fish with a straight lateral line (figure 4.1*a*) would have difficulty to determining the depth of a neighbor through hydrodynamic sensing. How this affects the responds to this neighbor is unclear. Fish with a two-dimensional lateral line, e.g. a lateral line that curves alongside the body of a fish (figure 4.1*b*), should have less trouble localizing neighboring conspecifics on a different depth. Although, even a curved lateral line

system seems more specialized in detecting waves in anterior/posterior direction rather than the vertical direction as only a small percentage of the lateral line canal is perpendicular to the movement direction. The superficial neuromasts, that are in most species dispersed over the body of the fish, are mainly used for sensing constant water currents and not sensing water accelerations induced by other animals [35].

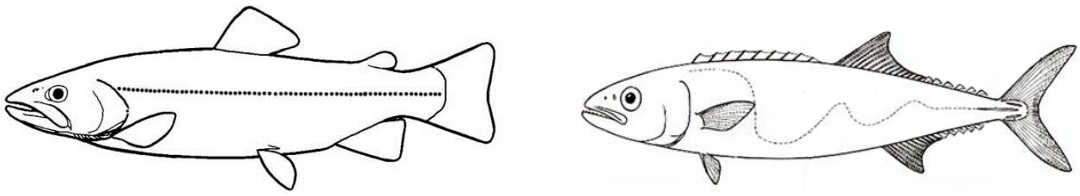

(a) Straight lateral line ***(b)*** Curved lateral line

Figure 4.1: Two different shapes of the lateral line systems. A curved lateral line presumably enables fish to better localize vibration sources in the vertical directions.

It could be that hydrodynamic waves coming from above produce less water displacement in the lateral line canals, because the openings of the canal are positioned at the side of the fish. This could would make vertical neighbors harder to perceive. Studies that measure excitation patterns of sensors in the lateral line canals, like Coombs [13] and Ćourčić-Blake and van Netten [17], vary the location of the vibrating source that produces hydrodynamic waves only in a horizontal plane. New studies are therefore needed that measure excitation patterns in the canal neuromasts produced by a vibrating source at various *vertical* positions to verify whether sensors in a lateral line canal react differently to vertical cues.

The shapes used in this study were not tweaked to fit empirical data. Future work might therefore consist of optimizing the shapes of behavioral zones to fit schooling data including measurements which were omitted from this research, such as: frontal density, polarization, nearest neighbor distance distributions (including 2nd and 3rd nearest neighbors) and nearest neighbor distance per bearing and elevation angle.

This present research is a mechanistic, rather than a functional, approach. However, swimming in a schools serves obviously several functions: it saves energy through wake exploitation [50], minimizes risk of getting eaten [36] and increases accuracy of navigation by means of the 'many-wrongs principle' [49, 12]. Bumann et al. suggest that the typical oblong school shape of fish could be the result of anti-predation strategies [8]. As it is now clear that the shape of the behavioral zones have a big influence on school shape and structure, future studies could therefore investigate the functional aspects of shape of behavioral zones and the corresponding shapes of the schools.

The present study only tested ellipsoidal shapes of behavioral zones, as this is mathematically easy to implement. A capsule-shaped behavioral zone might better reflect sensory capabilities considering the lateral line system can detect the location of a vibrating source one body-length away from any point of the lateral line [17], although we expect that this will have little effect on the shape and structure on the schools.

Besides changing the shape one could also add different weights or probability functions to the behavioral zones. This would make it possible that neighbors in a certain direction would

have a smaller influence or lower probability to be detected. The results from this study suggest that this will bring about similar patterns as can be obtained by changing the shape of behavioral zones. A stronger influence or higher probability to perceive another individual in a certain direction will lead to more spacing forces in the corresponding direction followed by a change in school shape and structure.

The current model theoretically allows agents to come very close to each other, as the agents are represented by points and do not possess real bodies. Having a rigid body would enable collisions which could provide the agents with free alignment [48], though collisions rarely occur in most species [37]. A real body would additionally lead to a change in perception of other agents. Agents perceive neighbors as closer when they have a body than when they are represented by points [34]. Further, a body is needed to implement real sensory obstruction. Currently, a phenomenological implementation is used. Namely the behavioral zones shrink when the local density perceived by an agent increases. Real sensory obstruction would mean that agents swimming behind the first row of neighbors are less often perceived. This would make interactions more localized and, in addition, the shape of the behavioral zones would form dynamically as a result of the obstruction by neighboring agents. The predefined shape of behavioral zones would thus have less influence on the shape and structure of the schools. A generic fish body would result in more occlusion of lateral, rather than frontal, neighbors. The width is generally much smaller than the length of a fish. This implies that an agent would perceive more agents in front than at his sides, which presumably would lead to interactions comparable to those found with Long behavioral zones.

The implications of the present study reach further than the schooling behavior in fish. Similar interaction rules are used in models of birds [26], pedestrians [22], locusts [4] and wildebeests [15]. Different shapes of behavioral zones could therefore be used to bring about swarm shapes or structures found in aggregations of other animals. The mechanisms in the present model are easy to extrapolate because fish are neutrally buoyant and thus do not need much additional rules like flight dynamics and roost attraction in starlings [26] to bring about realistic group behavior. The pitch angle correction (equation 2.18) is the only rule specific for fish schools. Removing this rule would merely cause more fluctuation in the pitch angle of agents and the schools.

The knowledge concerning the relation between the shapes of behavioral zones and the spatial structure of a swarm or school could be used to build a control mechanism for groups of autonomous vehicles based on self-organization. Many proposed control mechanisms can adjust the shape of the school to a particular group shape by first calculating the relative position of all the agents [5], or just of the agents at the periphery [32], in relation to the desired group shape. Afterwards the agents move until they occupy the correct positions to form the desired group shape. Cheng et al. proposed a control mechanism that can induce a swarm of identical agents to take up any two dimensional shape [11]. These proposed mechanisms rely on the fact that the agents can determine their relative positions with respect to the rest of all the agents in the group. This can take a long time and can be very computationally expensive, especially if a large number of agents is involved.

We show that the shape of a group, or in our case, a school of agents can be controlled *without* the agents knowing their position relative to the whole group, i.e. they only see their neighbors. The schools are polarized and the agents all swim upright, i.e. with their dorsal

side directed upwards. Hence a consensus between the agents about what the forward and up direction is has emerged out of the behavioral rules. This allows the school to adopt simple shapes, e.g. oblong, wide, flat school shapes, by changing the shape of the behavioral zones.

4.1 Summary

In sum, the present study shows that the shape of behavioral zones greatly affects school shape and structure in a predictable manner. School shape generally adopts, or exaggerates, the shape of behavioral zones. Schools brought about by Spherical and Flat behavioral zones are oblong even though the behavioral zones are not, due to the fact that these agents have a higher tendency to decelerate rather than steer to avoid neighbors. A phase transition has been found in runs with Long behavioral zones. Depending on the packing density of the school, Long behavioral zones can give rise to very oblong schools or oblong schools with densely packed slices throughout the width and height of the school.

With a cohesion weight of 9 $BL^2\,BM/s^2$ the position of the nearest neighbor, i.e. the bearing and elevation angle, is mainly induced by the blind angle. The shape of the behavioral zones, however, becomes the most influential factor when the attraction between the individual is lowered to 7 $BL^2\,BM/s^2$. The nearest neighbor is than most often located where the separation zones is smallest. Flat behavioral zones bring about the most natural schools, since the school shapes, bearing and elevation angles in schools brought about by Flat behavioral zones are repeatedly observed in empirical studies.

Bibliography

[1] I. Aoki. A simulation study on the schooling mechanism in fish. *Bull. Jap. Soc. Sci. Fish.*, 48:1081–1088, —1982—.

[2] B.E. Axelsen, T. Anker-Nilssen, P. Fossum, C. Kvamme, and L. Nøttestad. Pretty patterns but a simple strategy: predator-prey interactions between juvenile herring and Atlantic puffins observed with multibeam sonar. *Canadian Journal of Zoology*, 79(9):1586–1596, 2001.

[3] M. Ballerini, N. Cabibbo, R. Candelier, A. Cavagna, E. Cisbani, I. Giardina, V. Lecomte, A. Orlandi, G. Parisi, A. Procaccini, M. Viale, and V. Zdrakoviv. Interaction ruling animal collective behaviour depends on topological rather than metric distance: evidence from a field study. *PNAS*, 105(4):1232–1237, 2008.

[4] S. Bazazi, J. Buhl, J.J. Hale, M.L. Anstey, G.A. Sword, S.J. Simpson, and I.D. Couzin. Collective motion and cannibalism in locust migratory bands. *Current Biology*, 18(10):735–739, 2008.

[5] C. Belta and V. Kumar. Abstraction and control for groups of robots. *Robotics, IEEE Transactions on*, 20(5):865 – 875, 2004.

[6] D. Bodznick, J.C. Montgomery, and D.J. Bradley. Suppression of common mode signals within the electrosensory system of the little skate Raja erinacea. *Journal of Experimental Biology*, 171(1):107, 1992.

[7] C.M. Breder. Studies on social groupings in fishes. *Bulletin of the American Museum of Natural History*, 117:397–481, 1959.

[8] D. Bumann, J. Krause, and D. Rubenstein. Mortality risk of spatial positions in animal groups: the danger of being in the front. *Behaviour*, 134:1063–1076, —1997—.

[9] R. Cassinis, G. Bianco, A. Cavagnini, and P. Ransenigo. Strategies for navigation of robot swarms to be used in landmines detection. In *Proceeding of the Third European Workshop on Advanced Mobile Robots*, 1999.

[10] A. Cavagna, I. Giardina, A. Orlandi, G. Parisi, and A. Procaccini. The STARFLAG handbook on collective animal behaviour: 2. Three-dimensional analysis. *Animal Behaviour*, 76(1):237–248, 2008.

[11] J. Cheng, W. Cheng, and R. Nagpal. Robust and self-repairing formation control for swarms of mobile agents. In *Proceedings of the National Conference on Artificial Intelligence*, volume 20, page 59. Menlo Park, CA; Cambridge, MA; London; AAAI Press; MIT Press; 1999, 2005.

[12] E.A. Codling, J.W. Pitchford, and S.D. Simpson. Group navigation and the "many-wrongs principle" in models of animal movement. *Ecology*, 88(7):1864–1870, —2007—.

[13] S. Coombs, M. Hastings, and J. Finneran. Modeling and measuring lateral line excitation patterns to changing dipole source locations. *Journal of Comparative Physiology A: Neuroethology, Sensory, Neural, and Behavioral Physiology*, 178(3):359–371, 1996.

[14] I. D. Couzin, J. Krause, R. James, G. D. Ruxton, and N. R. Franks. Collective memory and spatial sorting in animal groups. *Journal of Theoretical Biology*, 218(1):1–11, —2002—.

[15] I.D. Couzin and J. Krause. Self-organization and collective behavior in vertebrates. *Advances in the Study of Behavior*, 32(1), 2003.

[16] J.M. Cullen. Methods for measuring the three-dimensional structure of fish schools. *Animal Behaviour*, 13:534–543, —1965—.

[17] B. Ćurčić-Blake and S.M. van Netten. Source location encoding in the fish lateral line canal. *Journal of Experimental Biology*, 209(8):1548, 2006.

[18] E.J. Denton and J. Gray. Mechanical factors in the excitation of clupeid lateral lines. *Proceedings of the Royal Society of London. Series B, Biological Sciences*, 218(1210):1–26, 1983.

[19] H. Edelsbrunner and E.P. Mücke. Three-dimensional alpha shapes. *ACM Transactions on Graphics*, 13:43–72, —1994—.

[20] A. Flock and J. Wersall. A study of the orientation of the sensory hairs of the receptor cells in the lateral line organ of fish, with special reference to the function of the receptors. *Journal of Cell Biology*, 15(1):19, 1962.

[21] R. Goldman. Intersection of two lines in three-space. In *Graphics gems*, page 304. Academic Press Professional, Inc., 1990.

[22] D. Helbing, P. Molnar, I.J. Farkas, and K. Bolay. Self-organizing pedestrian movement. *Environment and Planning B*, 28(3):361–384, 2001.

[23] C.K. Hemelrijk and H. Hildenbrandt. Self-organized shape and frontal density of fish schools. *Ethology*, 114:245–254, —2008—.

[24] C.K. Hemelrijk and H. Hildenbrandt. Personal communication. —2010—.

[25] C.K. Hemelrijk and H. Kunz. Density distribution and size sorting in fish schools: an individual-based model. *Behavioral Ecology*, 16(1):178, 2005.

[26] H. Hildenbrandt, C. Carere, and C.K. Hemelrijk. Self-organised complex aerial displays of thousands of starlings: a model. *Arxiv preprint arXiv:0908.2677*, 2009.

[27] A. Huth. *Ein Simulationsmodell zur Erklrung der Kooperativen Bewegung von polarisierten Fischschwrmen.* Ph. d., University Marburg, 1992.

[28] A. Huth and C. Wissel. The simulation of the movement of fish schools. *Journal of Theoretical Biology*, 156(3):365–385, —1992—.

[29] A. Huth and C. Wissel. The simulation of fish schools in comparison with experimental data. *Ecological Modelling*, 75/76:135–145, —1994—.

[30] P.J. Jarman. Prospects for interspecific comparison in sociobiology. *Current problems in sociobiology*, pages 323–342, 1982.

[31] B.A. Kadrovach and G.B. Lamont. A particle swarm model for swarm-based networked sensor systems. In *Proceedings of the 2002 ACM symposium on Applied computing*, pages 918–924. ACM New York, NY, USA, 2002.

[32] S. Kalantar and U.R. Zimmer. Distributed shape control of homogeneous swarms of autonomous underwater vehicles. *Autonomous Robots*, 22(1):37–53, 2007.

[33] R. Kawabe, Y. Naito, K. Sato, K. Miyashita, and N. Yamashita. Direct measurement of the swimming speed, tailbeat, and body angle of Japanese flounder (Paralichthys olivaceus). *ICES Journal of Marine Science*, 61(7):1080, 2004.

[34] H.P. Kunz and C. K. Hemelrijk. Artificial fish schools: collective effects of school size, body size, and body form. *Artificial Life*, 9(3):237–253, —2003—.

[35] J.C. Montgomery, C.F. Baker, and A.G. Carton. The lateral line can mediate rheotaxis in fish. *Nature*, 389(6654):960–963, 1997.

[36] J.K. Parrish. Re-examining the selfish herd: Are central fish safer?. *Animal Behaviour*, 38(6):1048–1053, 1989.

[37] B. L. Partridge. The structure and function of fish schools. *Scientific American*, 246(6):114–123, —1982—.

[38] B. L. Partridge, J. Johansson, and J. Kalish. The structure of schools of giant bluefin tuna in cape cod bay. *Environmental Biology of Fishes*, 9(3-4):253–262, 1983.

[39] B. L. Partridge, T. Pitcher, J. M. Cullen, and J. Wilson. The 3-dimensional structure of fish schools. *Behavioral Ecology and Sociobiology*, 6(4):277–288, —1980—.

[40] B. L. Partridge and T. J. Pitcher. The sensory basis of fish schools - relative roles of lateral line and vision. *Journal of Comparative Physiology*, 135(4):315–325, —1980—.

[41] T. J. Pitcher. 3-dimensional structure of schools in minnow, phoxinus-phoxinus (l). *Animal Behaviour*, 21(NOV):673–686, —1973—.

[42] T.J. Pitcher and B.L. Partridge. Fish school density and volume. *Marine Biology*, 54(4):383–394, 1979.

[43] C. W. Reynolds. Flocks, herds and schools: a distributed behavioral model. *Compter Graphics*, 21:25–36, —1987—.

[44] P. Romanczuk, I.D. Couzin, and L. Schimansky-Geier. Collective motion due to individual escape and pursuit response. *Physical Review Letters*, 102(1):10602, 2009.

[45] E. Sahin, T.H. Labella, V. Trianni, J.L. Deneubourg, P. Rasse, D. Floreano, LM Gambardella, F. Mondada, S. Nolfi, and M. Dorigo. Swarm-bot: Pattern formation in a swarm of self-assembling mobile robots. In *Proceedings of the IEEE International Conference on Systems, Man and Cybernetics, Hammamet, Tunisia*. Citeseer, 2002.

[46] J.K. Song and R.G. Northcutt. Morphology, distribution and innervation of the lateral-line receptors of the Florida gar, Lepisosteus platyrhincus. *Brain, behavior and evolution*, 37(1):10, 1991.

[47] W.M. Spears, D.F. Spears, J.C. Hamann, and R. Heil. Distributed, physics-based control of swarms of vehicles. *Autonomous Robots*, 17(2):137–162, 2004.

[48] J. Starruß, T. Bley, L. Søgaard-Andersen, and A. Deutsch. A new mechanism for collective migration in Myxococcus xanthus. *Journal of Statistical Physics*, 128(1):269–286, 2007.

[49] J. Surowiecki. *The Wisdom of Crowds*. Doubleday, —2004—.

[50] J.C. Svendsen, J. Skov, M. Bildsoe, and J.F. Steffensen. Intra-school positional preference and reduced tail beat frequency in trailing positions in schooling roach under experimental conditions. *Journal of Fish Biology*, 62(4):834–846, 2003.

[51] G. Weiss. *Multiagent systems: a modern approach to distributed artificial intelligence*. The MIT press, 2000.

Appendix A

Appendix

A.1 Calculations radii behavioral zones

To study the influence of shape of the behavioral zones of the agents, six different shapes are tested against the standard shape (Spherical). The volume of each separation, alignment and cohesion zone will have to be equal for each different shape in order to produce comparable data.

The behavioral zones are either spherical or ellipsoidal. The difficult part lies in calculating the volume of the blind area, which is not part of the behavioral zone as the agent do not respond to agents in their blind angle. All the agents have the same blind angle, but the volume of the blind area changes as the shape of the behavioral zones changes and thus the volume (of the active part) of the behavioral zones as well. We need to adjust the radii of the behavioral zones of the agents to match the volumes. Compensating by altering the blind angles is not favorable, since a difference in blind angle will result in different behavior, which makes it harder to investigate the influence of the shape.

$$Volume_{zone}(a,b,c) \quad = \quad \frac{4}{3}\pi\, a\, b\, c - Volume_{blind-area}(a,b,c) \tag{A.1}$$

The blind-area is essentially a cone with its tip at the center of the behavioral zones. We are interested in the volume of the blind-area ($Volume_{blind-area}$) which lies within the ellipsoid. Calculating the volume of an ellipsoid with a blind angle is more complicated than of a sphere because an ellipsoid can have three unequal radii. Equation A.1 shows the general equation we need to work out, where a, b and c are the radii of the ellipsoid. In this chapter the volume calculations for ellipsoids, however the same equations can be used to calculate the volume of a sphere will be discussed. In explaining the calculations two cases are distinguished, ellipsoids with equal width and height ($b == c$) and ellipsoids with unequal width and height ($b \neq c$).

Figure A.1 shows a horizontal and vertical cross-section of an ellipsoid. These sections are obtained by splitting the ellipsoid in half through radius a. In this case the width (b) of the ellipsoid is unequal to the height (c). This means that the blind area intersects the surface of the ellipsoid at different x-values, from $x1$ to $x2$. The volume of the blind area is therefore the sum of the volume of parts I, II and III. Note, that if the width of the ellipsoid would be equal to the height ($b == c$) part II would not be needed, considering the blind area would intersect with the surface at the same x-value ($x1$) in both the horizontal and vertical cross-section.

First, the x-values of the intersections points $x1$ and $x2$ are calculated by solving the equations for an ellipse A.2 and a sloped line A.3 with angle α representing the blind angle.

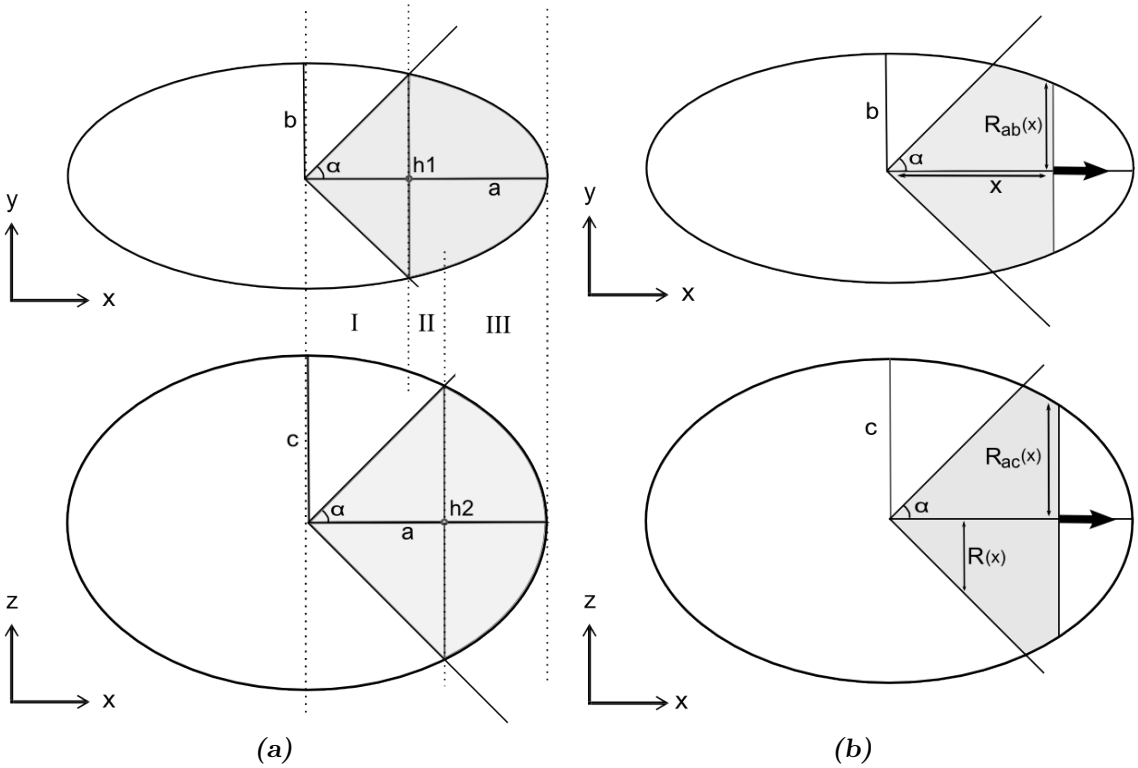

Figure A.1: (a) A horizontal (upper figure) and vertical (lower figure) cross-section of a ellipsoidal behavioral zone obtained by the splitting the ellipsoid in half through radius a. (b) The same cross-sections, but now with the direction of the integration indicated.

$$\frac{x^2}{a^2} + \frac{y^2}{b^2} = 1 \tag{A.2}$$

$$y = x \tan(\alpha) \tag{A.3}$$

$$x1(a,b) = \frac{b\,a}{\sqrt{b^2 + tan(\alpha)^2\,a^2}} \tag{A.4}$$

$$x2(a,c) = \frac{c\,a}{\sqrt{c^2 + tan(\alpha)^2\,a^2}} \tag{A.5}$$

$$R_{ab}(a,b,x) = \frac{\sqrt{-x^2 + a^2}b}{a} \tag{A.6}$$

$$R_{ac}(a,c,x) = \frac{\sqrt{-x^2 + a^2}c}{a} \tag{A.7}$$

The volume of the blind area can be obtained by integrating separately over the three parts, or two parts if $b == c$.

$$Volume_{blind-area} = Volume_{part-I} + Volume_{part-II} + Volume_{part-III} \tag{A.8}$$

Part-I runs from the center of the ellipsoid until the projection of the first intersection point $x1$ (figure A.1). Cross-sections of part-I through a are circles which grow in size as the cross-section is obtained closer to $x1$. Part-I is thus a cone which lies inside the ellipsoid. The radii of the circles (R) depends on the blind angle (α) and the distance (x) from the center point of the ellipsoid. We integrate using the surface of these circles ($S_{circles}$).

$$R(x) = x\,tan\,\alpha \tag{A.9}$$

$$S_{circle}(x) = R(x)\,R(x)\,\pi \tag{A.10}$$

$$Volume_{part-I} = \int_0^{x1} S_{circle}(x)\,dx \tag{A.11}$$

$$= \int_0^{x1} x^2\,(\tan\alpha)^2\,\pi\,dx$$

As mentioned before, we only need to calculate the volume of Part II if the width and height of the ellipsoid are unequal ($b \neq c$). Part II on the whole has an unusual shape, though we can calculate the surface ($S_{cross-section}$) of the cross-sections (figure A.2) as it consists of four simpler parts: two parts are a segment of a circle ($S_{circle-seg}$) and two parts are a segment of a ellipse ($S_{ellipse-seg}$). We need to calculate the angle $\phi(x)$ in order to determine how big the proportion of the segments are.

$$P_y(a,b,c,x) = R_{ac}(a,c,x)\sqrt{\frac{R(x)^2 - R_{ab}(a,b,x)^2}{R_{ac}(a,c,x)^2 - R_{ab}(a,b,x)^2}} \tag{A.12}$$

$$P_z(a,b,c,x) = R_{ab}(a,b,x)\sqrt{\frac{R_{ac}(a,c,x)^2 - R(x)^2}{R_{ac}(a,c,x)^2 - R_{ab}(a,b,x)^2}} \tag{A.13}$$

$$\phi(a,b,c,x) = \arctan\left(\frac{P_y(a,b,c,x)}{P_z(a,b,c,x)}\right) \tag{A.14}$$

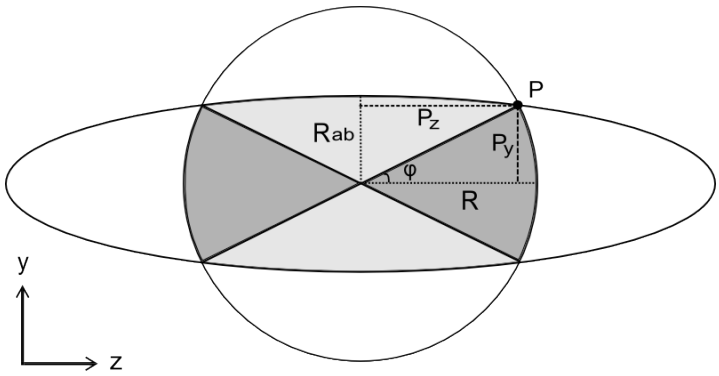

Figure A.2: A cross-section of part II. The summed surfacesof the gray parts in the figure is the area we want to integrate over. The darker gray parts have the shape of a segment of a ellipse ($S_{ellipse-seg}$) and the lighter gray parts have the shape of a segment of a circle ($S_{circle-seg}(x)$)

Equations A.15 and A.16 give the area of the circle and ellipse segments respectively. We have two pieces of each segment (figure A.2), hence the sum of the both segments times two gives us the area of the cross-sections. To obtain the volume of Part II we use the surface of the cross-section to integrate from $x1$ to $x2$ (figure A.1*(a)*).

$$S_{circle-seg}(a,b,c,x) = R(x)^2\phi(a,b,c,x) \tag{A.15}$$

$$S_{ellipse-seg}(a,b,c,x) = R_{ab}\,R_{ac}\arctan\left(\frac{R_{ab}\tan\left(\frac{1}{2}\pi-\phi\right)}{R_{ac}}\right) \tag{A.16}$$

$$S_{cross-section}(a,b,c,x) = 2\,S_{circle-seg}(a,b,c,x) + 2\,S_{ellipse-seg}(a,b,c,x) \tag{A.17}$$

$$Volume_{part-II} = \int_{x1}^{x2} S_{cross-section}(a,b,c,x)\,dx \tag{A.18}$$

To calculate the volume of part III of the ellipsoid, we have to obtain the volume of an ellipsoidal cap. A cross-section of part III will have the shape of an ellipse, or a circle when $b == c$. The ellipses will become smaller as x approaches the edge of the ellipsoid. We again integrate using the area of the cross-sections, we are therefore interested in the area of these ellipses. The radii of the ellipses are the perpendicular distance from a to the edge of the ellipsoid, thus R_{ab} and R_{ac} (figure A.1*b*).

$$S_{ellipse2}(a,b,c,x) = R_{ab}(a,b,c,x)\,R_{ac}(a,b,c,x)\,\pi \tag{A.19}$$

$$Volume_{part-III} = \int_{h2}^{a} S_{ellipse2}(a,b,c,x)\,dx \tag{A.20}$$

$$= \int_{x2}^{a} b\,c\left(1-\frac{x^2}{a^2}\right)\pi\,dx$$

The volume of the active part of an ellipsoidal behavioral response zone can thus be expressed as: [1]

[1] The Maple code of all the calculations are available on request

$$Volume_{zone} = \frac{4}{3}\pi abc - \int_0^{x1} R(x)R(x)\pi dx - \int_{x1}^{x2} S_{cross-section}(a,b,c,x)dx - \int_{x2}^{a} bc\left(1-\frac{x^2}{a^2}\right)\pi dx \tag{A.21}$$

A test application was written to check the equations. By generating a large number of points in a three dimensional space and comparing how many points were found inside and outside the behavioral zone we could approximate the volume of the behavioral zone. The approximated volume matched the volume which was calculated using the above equations.

A.2 School shapes with lower cohesion weight

Shape of BZ	Group size			
	50	**250**	**750**	**1500**
	L : W : H	L : W : H	L : W : H	L : W : H
Sphere	6.12 : 4.65 : 4.40	15.70 : 7.55 : 7.25	29.75 : 10.97 : 9.65	42.96 : 13.35 : 11.35
Wide	4.77 : 5.88 : 3.78	8.20 : 13.88 : 6.29	10.85 : 22.80 : 8.64	13.00 : 31.24 : 10.32
Narrow	7.38 : 3.85 : 4.25	16.53 : 6.96 : 7.63	24.17 : 9.91 : 12.15	27.46 : 10.99 : 16.67
High	4.69 : 3.94 : 6.05	8.30 : 6.19 : 13.91	11.10 : 8.82 : 22.40	13.41 : 10.74 : 30.24
Flat	8.56 : 6.03 : 2.16	17.51 : 11.48 : 2.91	30.23 : 19.76 : 3.88	42.13 : 28.43 : 4.24
Long	9.44: 4.50 : 3.33	20.01 : 7.83 : 5.22	21.77 : 9.88 : 7.80	23.35 : 12.02 : 10.98
Short	4.01 : 5.03 : 5.40	6.40 : 11.01 : 11.10	8.17 : 16.94 : 16.94	9.31 : 22.04 : 22.03

Table A.1: Average absolute Length, Width and Height of the school for all different shaped behavioral zones with a (low) cohesion weight of 7 $BL^2\,BM/s^2$. The school shapes found with cohesion weight of 7 $BL^2\,BM/s^2$ are similar to the shapes found with a cohesion weight 9 $BL^2\,BM/s^2$ (table 3.2).

A.3 Local density in schools

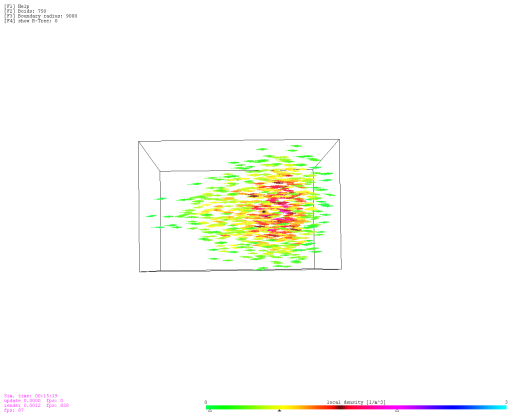

(a) High behavioral zones

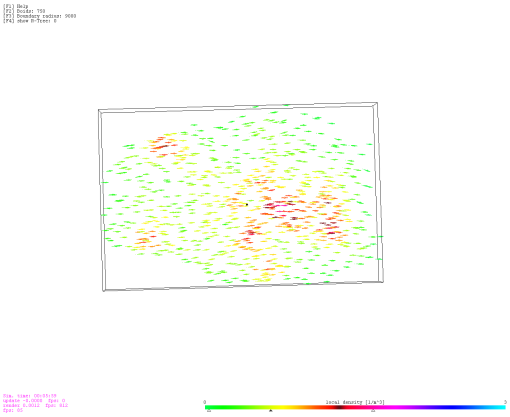

(b) Flat behavioral zones

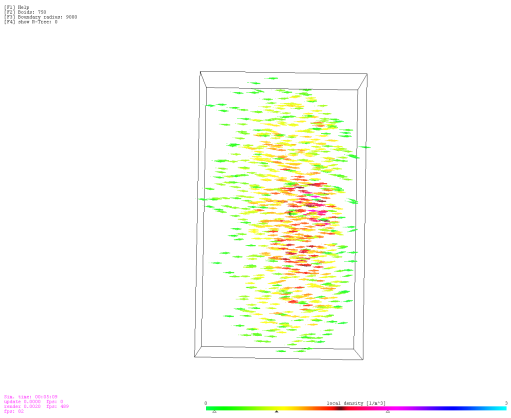

(c) Wide behavioral zones

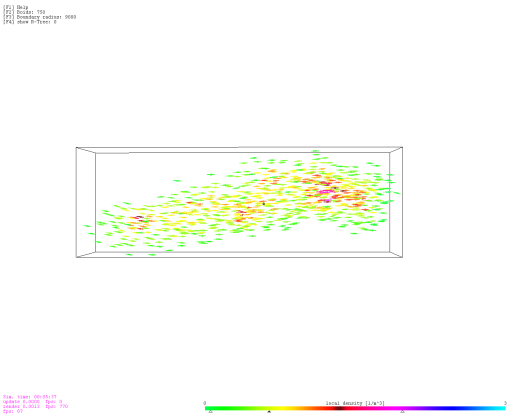

(d) Narrow behavioral zones

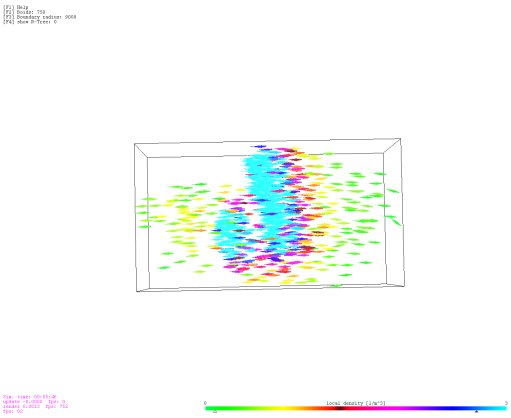

(e) Long behavioral zones

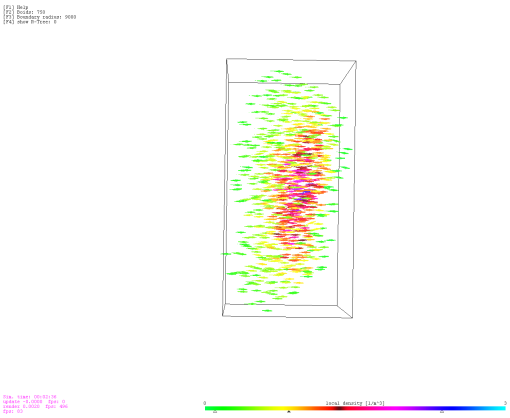

(f) Short behavioral zones

Figure A.3: Top-down view of the schools with respectively High, Flat, Wide, Narrow, Long and Short behavioral zones. The colors indicate the local density.

A.4 Increasing global density with group size

Shape BZ	Rank correlation coefficient	p	N
Sphere	0.607	< 0.001	36
High	0.683	< 0.001	36
Short	0.842	< 0.001	36
Flat	0.586	< 0.001	36
Long	0.745	< 0.001	36
Narrow	0.762	< 0.001	36
Wide	0.683	< 0.001	36

Table A.2: Results of Kendall's Tau rank correlation test (with adjustments for ties) for correlation between global density and group size. A significant positive correlation is found for all differently shaped behavioral zones.

Shape of BZ	Rank correlation coefficient	p	N
Sphere	-0.647	< 0.001	36
High	-0.878	< 0.001	36
Short	-0.810	< 0.001	36
Flat	-0.651	< 0.001	36
Long	-0.799	< 0.001	36
Narrow	-0.875	< 0.001	36
Wide	-0.878	< 0.001	36

Table A.3: Results of Kendall's Tau rank correlation test (with adjustments for ties) for correlation between NND and group size. A significant negative correlation is found for all differently shapes behavioral zones.

A.5 Density calculations without border individuals

To determine whether an individual is swimming at the periphery the centrality (C_i) of this individual regarding its neighbors is calculated. The centrality of an individual is obtained by calculating the vector-mean of the direction vectors to its neighbors within a range of twice the perception radius R_i.

$$C_i = \frac{1}{|N_c|} \left|\left| \sum_{j \epsilon N_c} d_{ij} \right|\right| \quad ; N_c = (j \epsilon N; d_{ij} \leq 2R_i) \tag{A.22}$$

C_i is close to zero when an individual is inside the aggregation and higher than 0.35 if the individual is on or near the periphery. Using these measures the individuals are classified as being on the periphery or in the interior (figure A.4).

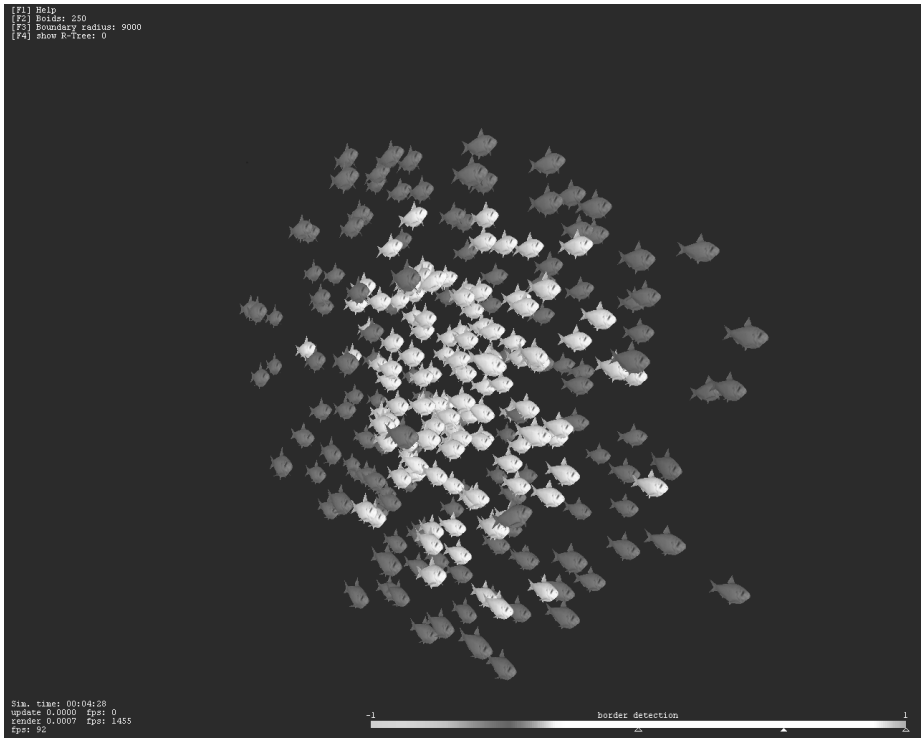

Figure A.4: A screen shot of a school. The darker individuals are classified as being on or near the periphery.

A.6 Packing density for inner individuals

Shape of BZ	Group size			
	50	**250**	**750**	**1500**
Sphere	15.1	138.5	497.4	1079
High	12.8	130.8	495.7	1090
Short	13.1	136.4	506.0	1101
Flat	13.7	108.9	373.0	788.1
Long	11.3	85.7	361.1	816.2
Narrow	13.2	121.4	465.8	1011
Wide	13.1	129.7	492.1	1022

(a)

Shape of BZ	Group size			
	50	**250**	**750**	**1500**
Sphere	0.302	0.554	0.663	0.719
High	0.256	0.523	0.661	0.727
Short	0.263	0.546	0.675	0.735
Flat	0.273	0.436	0.497	0.526
Long	0.226	0.343	0.482	0.544
Narrow	0.263	0.486	0.621	0.674
Wide	0.261	0.519	0.656	0.681

(b)

Table A.4: Results of runs in which the edge individuals were disregarded. *a)* #individuals in the inner part of (and not on the periphery of the) school per groupsize *b)* ratio #individuals in the inner part of the school divided by total #individuals

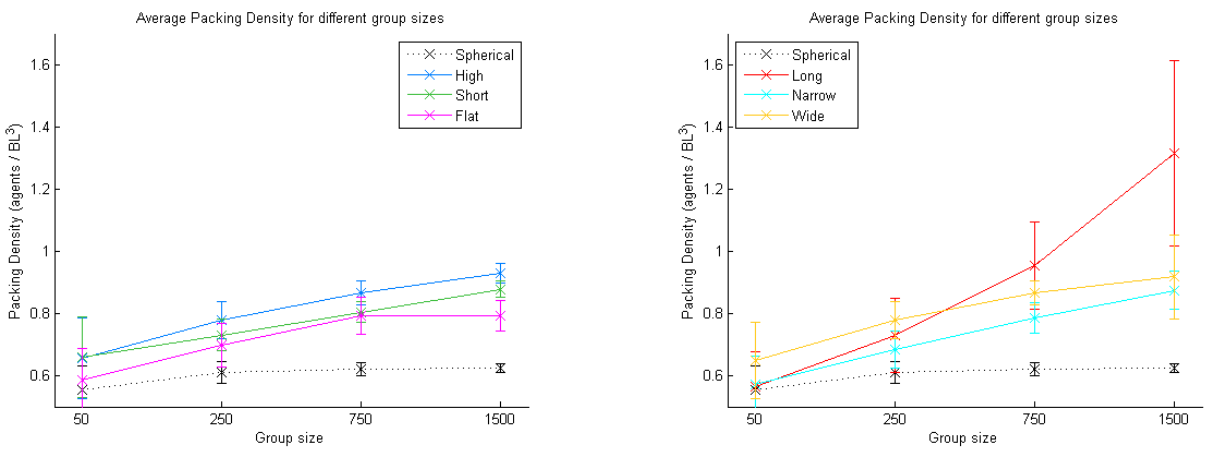

(a) ***(b)***

Figure A.5: The packing density (agent $/BL^3$) is plotted for the inner individuals of the school, disregarding the individuals on the periphery as they can produce a bias. The measurements are similar to packing densities where all the individuals are taken into account (figure 3.17).